Russell PA, Wainer Z, Wright GM, Daniels M, Conron M, Williams RA (2011) Does lung adenocarcinoma subtype predict patient survival?: a clinicopathologic study based on the new International Association for the Study of Lung Cancer/American Thoracic Society/European Respiratory Society international multidisciplinary lung adenocarcinoma classification. J Thorac Oncol 6(9):1496–1504. doi:10.1097/JTO.0b013e318221f701

Sica G, Yoshizawa A, Sima CS, Azzoli CG, Downey RJ, Rusch VW, Travis WD, Moreira AL (2010) A grading system of lung adenocarcinomas based on histologic pattern is predictive of disease recurrence in stage I tumors. Am J Surg Pathol 34(8):1155–1162. doi:10.1097/PAS.0b013e3181e4ee32

Su KY, Chen HY, Li KC, Kuo ML, Yang JC, Chan WK, Ho BC, Chang GC, Shih JY, Yu SL, Yang PC (2012) Pretreatment epidermal growth factor receptor (EGFR) T790M mutation predicts shorter EGFR tyrosine kinase inhibitor response duration in patients with non-small-cell lung cancer. J Clin Oncol 30(4):433–440. doi:10.1200/JCO.2011.38.3224

Takano T, Ohe Y, Sakamoto H, Tsuta K, Matsuno Y, Tateishi U, Yamamoto S, Nokihara H, Yamamoto N, Sekine I, Kunitoh H, Shibata T, Sakiyama T, Yoshida T, Tamura T (2005) Epidermal growth factor receptor gene mutations and increased copy numbers predict gefitinib sensitivity in patients with recurrent non-small-cell lung cancer. J Clin Oncol 23(28):6829–6837. doi:10.1200/JCO.2005.01.0793

Toyooka S, Matsuo K, Shigematsu H, Kosaka T, Tokumo M, Yatabe Y, Ichihara S, Inukai M, Suehisa H, Soh J, Kiura K, Fong KM, Lee H, Wistuba II, Gazdar AF, Mitsudomi T, Date H (2007) The impact of sex and smoking status on the mutational spectrum of epidermal growth factor receptor gene in non small cell lung cancer. Clin Cancer Res 13(19):5763–5768. doi:10.1158/1078-0432.CCR-07-0216

Travis WD, Brambilla E, Noguchi M, Nicholson AG, Geisinger KR, Yatabe Y, Beer DG, Powell CA, Riely GJ, Van Schil PE, Garg K, Austin JH, Asamura H, Rusch VW, Hirsch FR, Scagliotti G, Mitsudomi T, Huber RM, Ishikawa Y, Jett J, Sanchez-Cespedes M, Sculier JP, Takahashi T, Tsuboi M, Vansteenkiste J, Wistuba I, Yang PC, Aberle D, Brambilla C, Flieder D, Franklin W, Gazdar A, Gould M, Hasleton P, Henderson D, Johnson B, Johnson D, Kerr K, Kuriyama K, Lee JS, Miller VA, Petersen I, Roggli V, Rosell R, Saijo N, Thunnissen E, Tsao M, Yankelewitz D (2011) International association for the study of lung cancer/american thoracic society/european respiratory society international multidisciplinary classification of lung adenocarcinoma. J Thorac Oncol 6(2):244–285. doi:10.1097/JTO.0b013e318206a221

Tsuta K, Kozu Y, Mimae T, Yoshida A, Kohno T, Sekine I, Tamura T, Asamura H, Furuta K, Tsuda H (2012) c-MET/phospho-MET protein expression and MET gene copy number in non-small cell lung carcinomas. J Thorac Oncol 7(2):331–339. doi:10.1097/JTO.0b013e318241655f

Turke AB, Zejnullahu K, Wu YL, Song Y, Dias-Santagata D, Lifshits E, Toschi L, Rogers A, Mok T, Sequist L, Lindeman NI, Murphy C, Akhavanfard S, Yeap BY, Xiao Y, Capelletti M, Iafrate AJ, Lee C, Christensen JG, Engelman JA, Janne PA (2010) Preexistence and clonal selection of MET amplification in EGFR mutant NSCLC. Cancer Cell 17(1):77–88. doi:10.1016/j.ccr.2009.11.022

Wang W, Li Q, Yamada T, Matsumoto K, Matsumoto I, Oda M, Watanabe G, Kayano Y, Nishioka Y, Sone S, Yano S (2009) Crosstalk to stromal fibroblasts induces resistance of lung cancer to epidermal growth factor receptor tyrosine kinase inhibitors. Clin Cancer Res 15(21):6630–6638. doi:10.1158/1078-0432.CCR-09-1001

Warth A, Muley T, Meister M, Stenzinger A, Thomas M, Schirmacher P, Schnabel PA, Budczies J, Hoffmann H, Weichert W (2012) The novel histologic International Association for the Study of Lung Cancer/American Thoracic Society/European Respiratory Society classification system of lung adenocarcinoma is a stage-independent predictor of survival. J Clin Oncol 30(13):1438–1446. doi:10.1200/JCO.2011.37.2185

Yamada T, Takeuchi S, Kita K, Bando H, Nakamura T, Matsumoto K, Yano S (2012) Hepatocyte growth factor induces resistance to anti-epidermal growth factor receptor antibody in lung cancer. J Thorac Oncol 7(2):272–280. doi:10.1097/JTO.0b013e3182398e69

Yano S, Wang W, Li Q, Matsumoto K, Sakurama H, Nakamura T, Ogino H, Kakiuchi S, Hanibuchi M, Nishioka Y, Uehara H, Mitsudomi T, Yatabe Y, Sone S (2008) Hepatocyte growth factor induces gefitinib resistance of lung adenocarcinoma with epidermal growth factor receptor-activating mutations. Cancer Res 68(22):9479–9487. doi:10.1158/0008-5472.CAN-08-1643

J Cancer Res Clin Oncol (2013) 139:1869–1878
DOI 10.1007/s00432-013-1502-5

ORIGINAL PAPER

# Identification of prognostic immunophenotypic features in cancer stromal cells of high-grade neuroendocrine carcinomas of the lung

**Akiko Takahashi · Genichiro Ishii · Tomonari Kinoshita · Tatsuya Yoshida · Shigeki Umemura · Tomoyuki Hishida · Kiyotaka Yoh · Seiji Niho · Koichi Goto · Hironobu Ohmatsu · Yuichiro Ohe · Kanji Nagai · Atsushi Ochiai**

Received: 12 June 2013 / Accepted: 23 August 2013 / Published online: 7 September 2013


**Abstract**
*Purpose* The immunophenotypes of cancer stromal cells have been recognized as prognostic factors of cancer. The purpose of this study was to analyze the prognostic markers of high-grade neuroendocrine carcinomas of the lung (HGNEC; both small cell carcinoma and large cell neuroendocrine carcinoma) by examining the immunophenotypes of cancer stromal cells.
*Materials and methods* One hundred and fifteen patients who underwent a complete resection of HGNEC were included in this study. We examined the presence of CD204-positive tumor-associated macrophages (TAMs), Foxp3-positive regulatory T cells (Tregs), and podoplanin-positive cancer-associated fibroblasts (CAFs) to evaluate the prognostic values of these markers.
*Results* The number of CD204-positive TAMs and Foxp3-positive Tregs did not influence the overall survival (OS) or the relapse-free survival (RFS) of the patients. However, patients with podoplanin-positive CAFs had a significantly better prognosis than those with podoplanin-negative CAFs [OS: $p = 0.002$, RFS: $p = 0.002$, 5-year overall survival (5YR): 74 vs. 45 %]. According to subgroup analyses, patients with podoplanin-positive CAFs displayed a better prognosis for both small cell carcinoma (OS: $p = 0.046$, 5YR: 74 vs. 46 %) and large cell neuroendocrine carcinoma (OS: $p = 0.020$, 5YR: 74 vs. 45 %). Moreover, in multivariate analyses, the podoplanin status of the CAFs was shown to be a statistically significant independent predictor of recurrence.
*Conclusion* The presence of podoplanin-positive CAFs had a favorable prognostic value, suggesting that the evaluation of podoplanin expression by CAFs would lead to a novel risk classification of patients.

**Keywords** Small cell carcinoma · Large cell neuroendocrine carcinoma · High-grade neuroendocrine carcinomas · Cancer-associated fibroblasts · Tumor-associated macrophages · Regulatory T cells

**Electronic supplementary material** The online version of this article (doi:10.1007/s00432-013-1502-5) contains supplementary material, which is available to authorized users.

A. Takahashi · G. Ishii (✉) · T. Yoshida · A. Ochiai (✉)
Pathology Division, Department of Pathology, Research Center for Innovative Oncology, National Cancer Center Hospital East, 6-5-1, Kashiwanoha, Kashiwa-City, Chiba 277-8577, Japan
e-mail: gishii@east.ncc.go.jp

A. Ochiai
e-mail: aochiai@east.ncc.go.jp

A. Takahashi · T. Kinoshita · T. Yoshida · S. Umemura · T. Hishida · K. Yoh · S. Niho · K. Goto · H. Ohmatsu · Y. Ohe · K. Nagai
Department of Thoracic Oncology, National Cancer Center Hospital East, 6-5-1, Kashiwanoha, Kashiwa-City, Chiba 277-8577, Japan

## Introduction

The World Health Organization (WHO) currently classifies neuroendocrine tumors into four types: typical carcinoid (TC), intermediate-grade atypical carcinoid (AC), large cell neuroendocrine carcinoma (LCNEC), and small cell lung carcinoma (SCLC) (Travis et al. 1991). LCNEC and SCLC are categorized as high-grade neuroendocrine carcinomas (HGNEC) because of their poor prognoses, compared with the prognoses for TC and AC. Although some clinicopathological differences exist between LCNEC and SCLC, these tumor types have similar pathological

characteristics including a high mitotic rate, frequent necrosis, and neuroendocrine phenotype (Travis 2010). Several recent studies have reported that LCNEC responds to cisplatin-based chemotherapy in a manner similar to SCLC (Yamazaki et al. 2005; Rossi et al. 2005; Asamura et al. 2006; Igawa et al. 2010; Sun et al. 2012), and the survival of patients with LCNEC as well as those with SCLC who undergo surgery alone is relatively poor (Rossi et al. 2005; Iyoda et al. 2006; Sarkaria et al. 2011). Therefore, the identification of risk factors for these diseases is important for the development of novel therapies.

Cancer tissue is composed not only of cancer cells, but also of stromal cells such as fibroblasts (cancer-associated fibroblasts: CAFs), monocyte/macrophages (tumor-associated macrophages: TAMs), and immune cells (lymphocytes and neutrophils) (Bhowmick et al. 2004; Pollard 2004; Ding et al. 2012). Recently, the microenvironment surrounding cancer cells has become a focus of study, since cancer progression is not solely determined by the cancer cells themselves, but also by the surrounding stromal cells (Bhowmick et al. 2004; Pollard 2004; Ding et al. 2012).

Extensive clinical evidence and experimental mouse models have shown that certain types of CAFs and TAMs may have a tumor-promoting phenotype. We previously reported that CAFs expressing podoplanin were capable of enhancing the tumor formation rate, compared with podoplanin-negative CAFs, and that podoplanin-positive CAFs could be a prognostic factor in lung adenocarcinoma (Kawase et al. 2008; Hoshino et al. 2011; Ito et al. 2012a). As for TAMs, studies have shown a significant association between the number of CD204-positive macrophages and a poor outcome in several types of cancers (Ohtaki et al. 2010; Komohara et al. 2011; Kurahara et al. 2011). Regarding immune cells, recent studies have shown that the accumulation of immunosuppressive lymphocytes (represented by regulatory T cells: Tregs) is associated with advanced tumor growth and a poor outcome in several types of malignant tumors including lung cancers (Petersen et al. 2006; Shimizu et al. 2010; Chen and Oppenheim 2011; Tao et al. 2012; Wang et al. 2012). These results were supported by the observation that patients with a variety of cancers have enlarged pools of Tregs in their peripheral blood, tumor-draining lymph nodes, and the tumor itself (Koyama et al. 2008; Karagoz et al. 2010).

Clarification of the role of stromal cells as a prognostic factor may lead to a novel risk classification of patients and more effective treatment strategies. Previous reports have indicated the prognostic value of stromal cells in adenocarcinoma or non-small cell lung cancer (NSCLC); (Kawase et al. 2008; Ohtaki et al. 2010; Hoshino et al. 2011; Tao et al. 2012; Bremnes et al. 2011; Dimitrakopoulos et al. 2011); however, the prognostic value of stromal cells in completely resected HGNEC of the lung has not been previously reported. This study attempted to identify prognostic biological markers obtained from surgically resected HGNEC specimens by examining the immunophenotypes of cancer stromal cells, including TAMs, Tregs, and CAFs, with special attention to the expressions of CD204, Foxp3, and podoplanin, respectively. We anticipated that this study could lead to the development of a novel risk classification for patients and the realization of a new therapeutic strategy for the treatment of HGNEC.

## Materials and methods

### Patients

During the period from January 1993 to October 2011, a total of consecutive 131 patients with HGNEC of the lung underwent surgical resection at the National Cancer Center Hospital East, Chiba, Japan. Among these patients, 16 were excluded because their cancers were composed of two or more non-small cell carcinoma elements. The remaining 115 patients were included in this retrospective study. The median follow-up period of the patients was 4.4 years. The tumors were staged according to the seventh edition of the tumor–node–metastasis classification developed by the International Union Against Cancer. The survival period was measured from the date of surgery.

### Histological evaluation

Ten percent formalin or methanol-fixed and paraffin-embedded surgical specimens were collected from all the patients. The samples were cut at 5-mm intervals, and 4-μm sections were stained with hematoxylin and eosin (HE). Intratumoral vascular invasion and visceral pleural invasion were analyzed using HE and Verhoeff-van-Gieson staining methods. Two independent observers (A.T. and G.I.) who were unaware of the clinical data reviewed all the histological slides. Histological diagnosis of SCLC and LCNEC was made according to the third edition of the WHO guidelines. In this study, we selected the cases of SCLC which contained more than 50 % component of SCLC. As for LCNEC, we selected the cases with more than 50 % component of LCNEC.

### Immunohistochemistry

The 4-μm sections were deparaffinized in xylene and rehydrated in a graded alcohol series. After washing in distilled water, the slides were placed in 0.1M citric acid buffer. For antigen retrieval, the slides were heated twice at 95 % for 20 min in a microwave oven (H2800 Microwave Processor; Energy Beam Science, East Granby, CT, USA)

and then allowed to cool for one hour at room temperature. The slides were immersed in methanol containing 0.3 % hydrogen peroxide for 15 min to inhibit the endogenous peroxidase activity. Nonspecific binding was blocked by preincubation with 2 % normal swine serum in phosphate-buffered saline for 30 min at room temperature. Tissue sections were stained overnight at 4 °C with a mouse anti-human CD204 antibody (Scavenger Receptor Class A-E5; Transgenic, Japan) at a final dilution of 1: 400, anti-human Foxp3 antibody (ab20034 clone 236A/E7; Abcam Inc, Cambridge, MA, USA) at a final dilution of 1: 200, and anti-human podoplanin antibody (D2-40; Signet Laboratories, Dedham, MA, USA) at a final dilution of 1: 50. The slides were subsequently incubated with EnVision™ (DAKO, Denmark) for 1 h at room temperature. After extensive washing with PBS, the color reaction was developed in 2 % 3, 3′-diaminobenzidine in 50 mM Tris-buffer (pH 7.6) containing 0.3 % hydrogen peroxidase. Finally, the sections were counterstained with Meyer's hematoxylin, dehydrated, and mounted.

The 5 most CD204-positive TAMs-infiltrated areas within each section were selected, and the number of CD204-positive TAMs was counted under a light microscope at a ×400 magnification (0.0625 $mm^2$/field). The average count was recorded as the number of CD204-positive TAMs for each case. The 5 most Foxp3-positive Tregs-infiltrated areas were selected, and the number of Foxp3-positive Tregs was counted under a light microscope at a ×400 magnification (0.0625 $mm^2$/field). As for podoplanin expression in the CAFs, a specimen was judged as positive if at least 50 % of the fibroblasts showed an unequivocal reaction for podoplanin that was equal to that of lymphatic endothelial cells.

### Statistical analysis

Differences in categorical outcomes were evaluated using the chi-square test. Overall survival was defined as the period from the date of surgery until the date of death from any cause or the last date on which the patient was known to be alive. The length of the relapse-free period was calculated in months from the date of resection until the date of the first recurrence or the last follow-up. Overall survival and the relapse-free period were calculated using the Kaplan–Meier method, and the differences between the groups were analyzed using a log-rank test. Cox proportional hazards multivariate models were used to identify independent predictors. All the $p$ values that were reported were 2-sided, and the significance level was set at less than 0.05. Analyses were performed using the statistical software JMP 9. This study was conducted as part of a National Cancer Center institutional review board-approved protocol.

## Results

### Clinicopathological characteristics

Table 1 shows the clinicopathological characteristics of the patients. There were 98 men (85 %), and their median age at the time of surgery was 68 years (range 22–86 years); 71 patients had p-stage I diseases. The histologic type was SCLC in 52 patients and LCNEC in 63. 17 patients of SCLC and 24 patients of LCNEC had lymphatic invasion. Among the SCLC cases, the proportion of patients with p-T1 was significantly higher than that among the LCNEC cases. In this study, none of the patients were given neo-adjuvant chemotherapy.

**Table 1** Clinicopathological characteristics of the patients

| Characteristics | All cases | SCLC | LCNEC | $p$ value† |
|---|---|---|---|---|
| No. of patients | 115 | 52 | 63 | |
| Age (year) | | | | |
| <70 | 61 | 30 | 31 | |
| ≥70 | 54 | 22 | 32 | 0.364 |
| Gender | | | | |
| Female | 17 | 8 | 9 | |
| Male | 98 | 44 | 54 | 0.869 |
| Brinkman index | | | | |
| <1,000 | 60 | 31 | 29 | |
| ≥1,000 | 55 | 21 | 34 | 0.146 |
| pT | | | | |
| T1a–T1b | 46 | 30 | 16 | |
| T2a–T4 | 69 | 22 | 47 | <0.001* |
| pN | | | | |
| pN0 | 79 | 35 | 44 | |
| pN1–2 | 36 | 17 | 19 | 0.771 |
| Pathological stage | | | | |
| IA | 37 | 24 | 13 | |
| IB | 34 | 8 | 26 | |
| IIA–IV | 44 | 20 | 24 | 0.002* |
| Vascular invasion | | | | |
| Absent | 23 | 10 | 13 | |
| Present | 92 | 42 | 50 | 0.851 |
| Lymphatic invasion | | | | |
| Absent | 74 | 35 | 39 | |
| Present | 41 | 17 | 24 | 0.547 |
| Pleural invasion | | | | |
| Absent | 75 | 36 | 39 | |
| Present | 40 | 16 | 24 | 0.411 |

*SCLC* small cell lung carcinoma, *LCNEC* large cell neuroendocrine carcinoma

* Indicates significance, † chi-square test

### Immunohistochemical staining of CD204-positive TAMs, Foxp3-positive Tregs, and podoplanin-positive CAFs

Representative immunohistochemical staining results for CD204, Foxp3, and podoplanin are shown in Fig. 1. The median number of CD204-positive TAMs was 20 per 0.0625 $mm^2$, with a range of 1.5–93.8. Patients were classified into two groups based on the median number of CD204-positive TAMs in the entire group: a high CD204-positive TAMs group (>20/field) (Fig. 1a), or a low CD204-positive TAMs group (0–20/field) (Fig. 1b). The median number of Foxp3-positive Tregs was 6 per 0.0625 $mm^2$ (range 0.5–45.5). Similarly, patients were classified into two groups of Foxp3-positive Tregs (>5/field) (Fig. 1c, d). Cases with podoplanin-positive CAFs were identified in 47 (41 %) samples (Fig. 1e, f).

### Associations between clinicopathological factors and CD204-positive TAMs, Foxp3-positive Tregs, or podoplanin-positive CAFs

The associations between clinicopathological variables and the number of CD204-positive TAMs, Foxp3-positive Tregs, or podoplanin-positive CAFs are shown in Table 2. No differences in the clinicopathological variables were observed among the three groups.

### Evaluation of CD204-positive TAMs, Foxp3-positive Tregs, or podoplanin-positive CAFs as prognostic factors in patients with HGNEC

The number of CD204-positive TAMs and Foxp3-positive Tregs did not influence the overall survival (OS) or the relapse-free survival (RFS) period of the patients (Fig 2a–d). On the other hand, the OS and RFS of the patients with

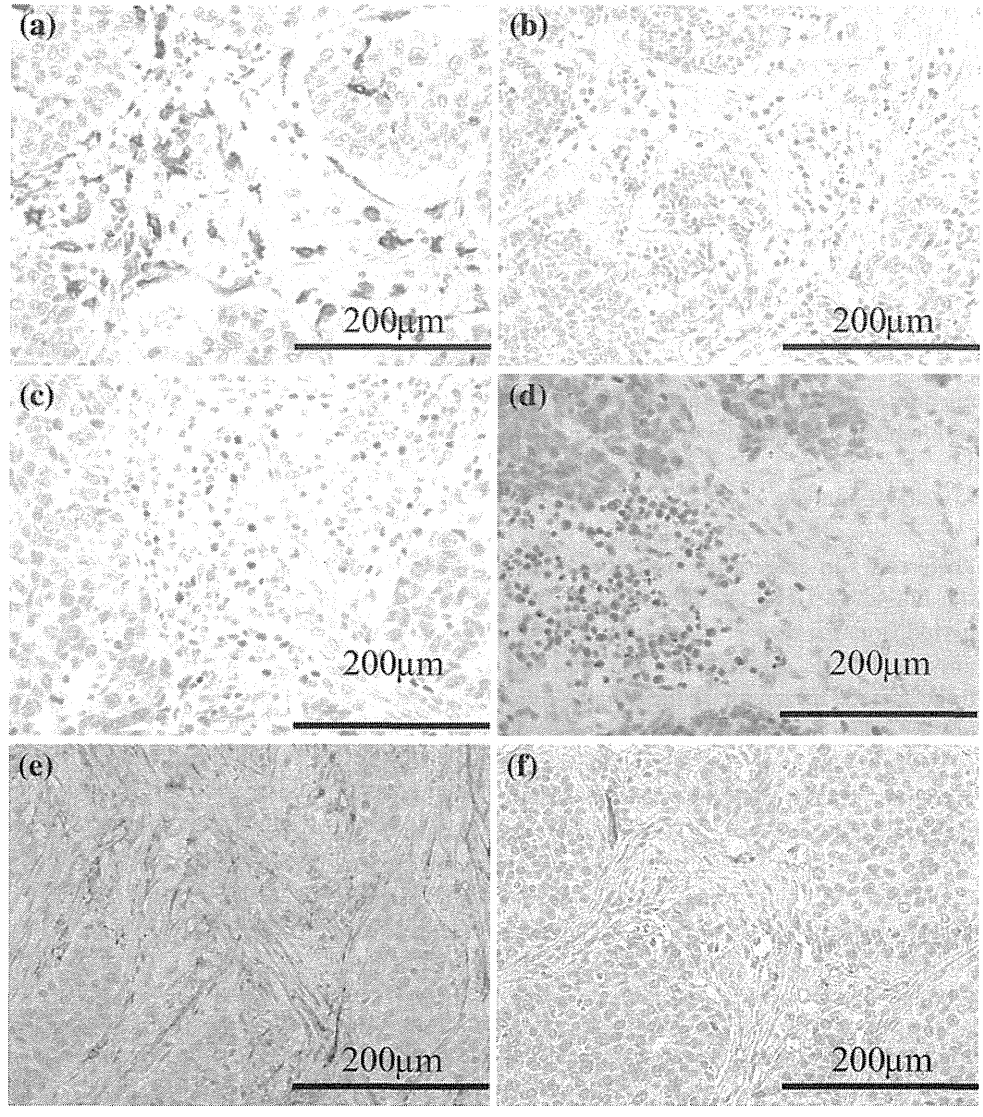


**Fig. 1** Immunohistochemical staining for CD204, Foxp3, and podoplanin in high-grade neuroendocrine carcinoma (HGNEC) of the lung. **a** A case with high CD204-positive tumor-associated macrophages (TAMs). **b** A case with low CD204-positive TAMs. **c** A case with high Foxp3-positive regulatory T cells (Tregs). **d** A case with low Foxp3-positive Tregs. **e** A case with podoplanin-positive cancer-associated fibroblasts (CAFs). **f** A case with podoplanin-negative CAFs

**Table 2** Correlation between CD204-positive TAMs, Foxp3-positive Tregs, podoplanin-positive CAFs, and clinicopathological factors

| Characteristics | No. of patients (%) | | *p* value* | No. of patients (%) | | *p* value* | No. of patients (%) | | *p* value* |
|---|---|---|---|---|---|---|---|---|---|
| | CD204 | | | Foxp3 | | | Podoplanin | | |
| | High ($n = 58$) | Low ($n = 57$) | | High ($n = 57$) | Low ($n = 58$) | | Positive ($n = 47$) | Negative ($n = 68$) | |
| Age (year) | | | | | | | | | |
| <70 | 26 (45) | 35 (61) | | 27 (47) | 34 (59) | | 20 (43) | 41 (60) | |
| ≥70 | 32 (55) | 22 (39) | 0.074 | 30 (53) | 24 (41) | 0.226 | 27 (53) | 27 (40) | 0.061 |
| Gender | | | | | | | | | |
| Female | 7 (12) | 10 (18) | | 7 (12) | 10 (17) | | 5 (11) | 12 (18) | |
| Male | 51 (88) | 47 (82) | 0.407 | 50 (88) | 48 (83) | 0.453 | 42 (89) | 56 (82) | 0.290 |
| Brinkman index | | | | | | | | | |
| <1,000 | 31 (53) | 29 (51) | | 27 (47) | 33 (57) | | 22 (47) | 38 (56) | |
| ≥1,000 | 27 (47) | 28 (49) | 0.783 | 30 (53) | 25 (43) | 0.306 | 25 (53) | 30 (44) | 0.338 |
| pT | | | | | | | | | |
| pT1a–pT1b | 19 (33) | 27 (47) | | 21 (37) | 25 (43) | | 18 (38) | 28 (47) | |
| pT2a–pT4 | 39 (47) | 30 (53) | 0.109 | 36 (63) | 33 (57) | 0.493 | 29 (62) | 40 (53) | 0.757 |
| pN | | | | | | | | | |
| pN0 | 40 (69) | 39 (68) | | 42 (73) | 37 (64) | | 36 (77) | 43 (63) | |
| pN1–2 | 18 (31) | 18 (32) | 0.950 | 15 (27) | 21 (36) | 0.252 | 11 (23) | 25 (37) | 0.125 |
| Pathological stage | | | | | | | | | |
| IA | 16 (28) | 21 (37) | | 19 (33) | 18 (31) | | 18 (38) | 19 (31) | |
| IB | 19 (32) | 15 (27) | | 18 (32) | 16 (28) | | 14 (30) | 20 (26) | |
| IIA–IV | 23 (40) | 21 (36) | 0.540 | 20 (35) | 24 (41) | 0.779 | 15 (32) | 29 (43) | 0.413 |
| Vascular invasion | | | | | | | | | |
| Absent | 10 (17) | 13 (23) | | 12 (21) | 11 (19) | | 12 (26) | 11 (16) | |
| Present | 48 (83) | 44 (77) | 0.455 | 45 (79) | 47 (81) | 0.780 | 35 (74) | 57 (84) | 0.221 |
| Lymphatic invasion | | | | | | | | | |
| Absent | 39 (67) | 35 (61) | | 41 (72) | 33 (57) | | 32 (68) | 42 (62) | |
| Present | 19 (33) | 22 (39) | 0.513 | 16 (28) | 25 (43) | 0.091 | 15 (32) | 26 (38) | 0.485 |
| Pleural invasion | | | | | | | | | |
| Absent | 40 (69) | 35 (61) | | 38 (67) | 37 (64) | | 33 (70) | 42 (62) | |
| Present | 18 (31) | 22 (39) | 0.394 | 19 (33) | 21 (36) | 0.746 | 14 (30) | 26 (38) | 0.348 |

* Chi-square test

podoplanin-positive CAFs were significantly longer than that of the patients with podoplanin-negative CAFs [$p = 0.002$ and $p = 0.002$, respectively; Fig. 2e and f; 5-year overall survival rate (5YR) 74 vs. 45 %]. We also analyzed a subgroup that did not receive postoperative chemotherapy ($n = 67$). Among this cohort, we found that patients with podoplanin-positive CAFs had a better outcome than the patients with podoplanin-negative CAFs (OS: $p = 0.003$, RFS: $p < 0.001$; Fig. 3).

Online Resource Fig. S1a and 1b showed the survival curves for the p-stage I patients. CD204-positive TAMs and Foxp3-positive Tregs did not influence the survival curves (data not shown); however, patients with podoplanin-positive CAFs had a significantly better prognosis than those with podoplanin-negative CAFs (OS, $p = 0.002$; RFS, $p = 0.002$; 5YR, 78 vs. 48 %). Online Resource Fig. S1c-f showed the OS and RFS for the SCLC and LCNEC cases. Podoplanin-positive CAFs were associated with a significantly better OS and RFS in both the SCLC and the LCNEC cases (SCLC 5YR, 74 vs. 46 %; LCNEC 5YR, 74 vs. 45 %).

## Univariate and multivariate analyses of factors associated with prognosis

A univariate analysis identified 4 significant risk factors for OS: sex (female), pN(+), lymphatic permeation (+), and podoplanin-negative CAFs (Table 3). In a multivariate

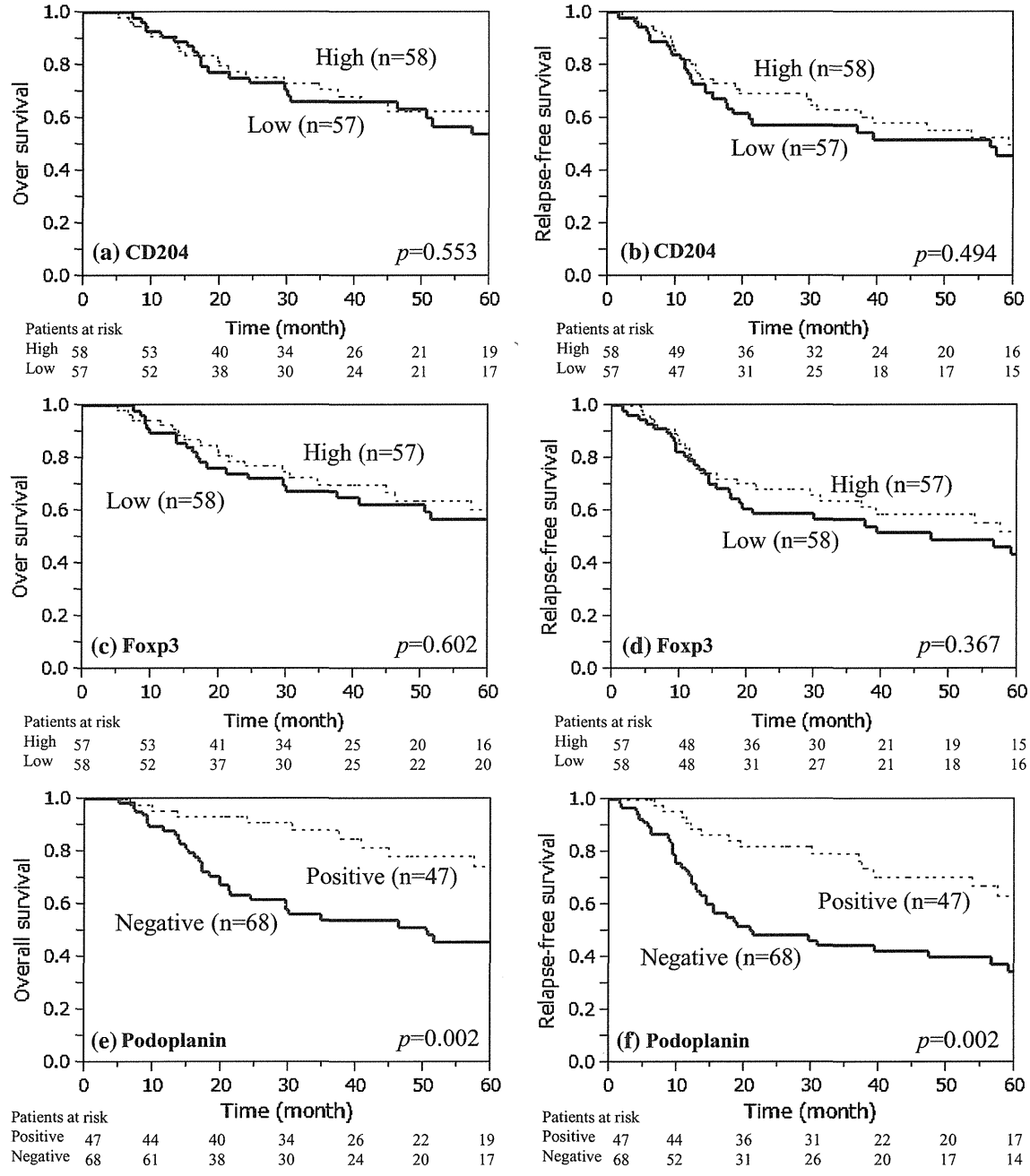


**Fig. 2** Survival analysis of HGNEC patients with CD204-positive TAMs, Foxp3-positive Tregs, and podoplanin-positive CAFs. **a** Overall survival curves according to CD204 expression in TAMs. **b** Relapse-free survival curves according to CD204 expression in TAMs. **c** Overall survival curves according to Foxp3 expression in Tregs. **d** Relapse-free survival curves according to Foxp3 expression in Tregs. **e** Overall survival curves according to podoplanin expression in CAFs. **f** Relapse-free survival curves according to podoplanin expression in CAFs

analysis using the Cox regression model, sex, the presence of lymphatic permeation (ly), and podoplanin-negative CAFs were shown to be statistically significant independent predictors for recurrence (Table 3A). Furthermore, the podoplanin status of the CAFs was an independent prognostic factor for the patients without postoperative chemotherapy (Table 3B).

## Subgroup analysis combining podoplanin-positive CAFs and other independent risk factors

We divided the HGNEC patients into 3 groups (Group A: ly (−)/podoplanin-positive CAFs; Group B: ly (+)/podoplanin-positive CAFs or ly (−)/podoplanin-negative CAFs; and Group C: ly (+)/podoplanin-negative CAFs).

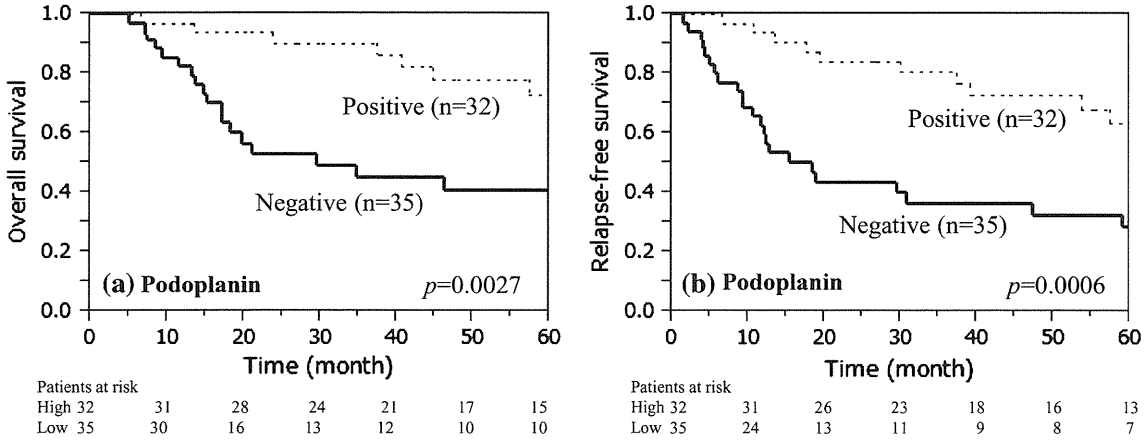


**Fig. 3** Survival analysis of HGNEC patients without postoperative chemotherapy. **a** Overall survival curves. **b** Relapse-free survival curves

**Table 3** Impact of potential prognostic factors on survival of patient in high-grade neuroendocrine carcinoma by univariate and multivariate analysis ($n = 115$)

| Variable | Univariate analysis, $p$ | Multivariate analysis | | |
|---|---|---|---|---|
| | | Hazard ratio | 95 % CI | $p$ |
| A | | | | |
| Pathology (SCLC) | 0.908 | – | – | – |
| Age (≥70 year) | 0.597 | – | – | – |
| Gender (female) | 0.031* | 2.296 | 1.050–4.631 | 0.038* |
| Brinkman index (≥1,000) | 0.796 | – | – | – |
| pT (pT2–pT4) | 0.900 | – | – | – |
| pN (pN1–2) | 0.011* | 1.388 | 0.704–2.736 | 0.341 |
| Vascular invasion (present) | 0.152 | – | – | – |
| Lymphatic invasion (present) | 0.002* | 2.435 | 1.242–4.862 | 0.010* |
| Pleural invasion (present) | 0.815 | – | – | – |
| CD204 (high-CD204 TAMs) | 0.553 | – | – | – |
| Foxp3 (high-Foxp3 Tregs) | 0.602 | – | – | – |
| Podoplanin [Podoplanin (−) CAFs] | 0.002* | 2.472 | 1.191–5.634 | 0.014* |
| B | | | | |
| Pathology (SCLC) | 0.479 | – | – | – |
| Age (≥70 year) | 0.249 | – | – | – |
| Gender (female) | 0.346 | – | – | – |
| Brinkman Index (≥1,000) | 0.862 | – | – | – |
| pT (pT2–pT4) | 0.721 | – | – | – |
| pN (pN1–2) | 0.003* | 2.088 | 0.866–4.883 | 0.099 |
| Vascular invasion (present) | 0.009* | 3.787 | 0.750–68.954 | 0.121 |
| Lymphatic invasion (present) | 0.002* | 2.316 | 0.993–5.577 | 0.052 |
| Pleural invasion (present) | 0.735 | – | – | – |
| CD204 (high-CD204 TAMs) | 0.497 | – | – | – |
| Foxp3 (high-Foxp3 Tregs) | 0.945 | – | – | – |
| Podoplanin [podoplanin (−) CAFs] | 0.003* | 2.423 | 1.015–6.422 | 0.046* |

* Indicates significance

*SCLC* small cell lung cancer, *TAMs* tumor-associated macrophages, *Tregs* regulatory T cells, *CAFs* cancer-associated fibroblasts

The overall survival curves of the three groups are shown in Fig. 4 (5YR: A, 78, B, 55, C, 35 %). Group A showed a significantly longer survival period than Group B ($p < 0.01$) or Group C ($p < 0.01$).

## Discussion

A few previous reports focusing on the immunophenotypes of the tumor cells have examined prognostic factors based

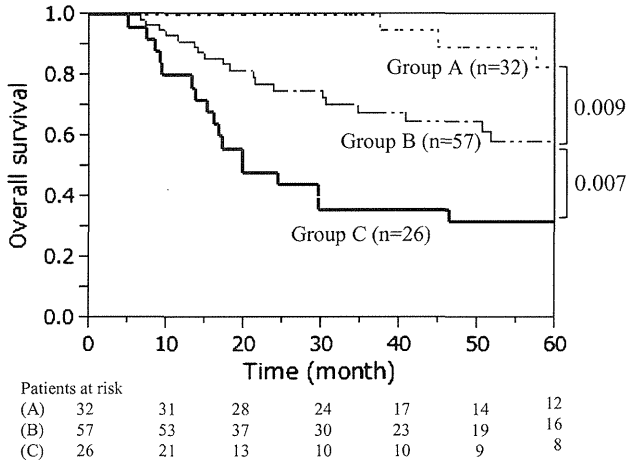


**Fig. 4** Subgroup analysis combining podoplanin expression in CAFs and other independent risk factors. Group A: ly (−)/podoplanin-positive CAFs; Group B: ly (+)/podoplanin-positive CAFs or ly (−)/podoplanin-negative CAFs; and Group C: ly (+)/podoplanin-negative CAFs)

on surgically resected HGNEC specimens (Usuda et al. 2011a, b; Erler et al. 2011; Ryuge et al. 2012). Recent studies have revealed that the immunophenotypes of not only cancer cells, but also cancer stromal cells can be useful as prognostic factors. So far, few reports have examined the prognostic significance of cancer stromal cells in surgically resected HGNEC. In the current study, we first clearly showed that the immunophenotypes of cancer stromal cells, especially CAFs, could be used as prognostic factors for patients with HGNEC.

In this study, the number of infiltrating CD204-positive TAMs and Foxp3-positive Tregs did not influence the outcome of the patients with HGNEC. We previously reported that a higher number of infiltrating CD204-positive TAMs was a predictor of an unfavorable prognosis in lung adenocarcinoma (Ohtaki et al. 2010). Moreover, Petersen et al. and Tao et al. also reported that Foxp3-positive Tregs were a predictor of an unfavorable prognosis in NSCLC (Petersen et al. 2006; Tao et al. 2012). As for SCLC also, Wang et al. showed that Foxp3-positive Tregs predict a poor prognosis (Wang et al. 2012). These results, which contradict the results of the present study, might have arisen from the fact that they used SCLC biopsy specimens, not surgically resected specimens of SCLC. Alternatively, their cohort included patients with advanced SCLC; thus, Tregs may play a role in advanced SCLC. Generally, tumor malignancy is influenced by several extrinsic factors within the cancer microenvironment as well as intrinsic factors in the cancer cells. The cancer cells of HGNEC have a higher malignant potential, including a higher proliferative activity and anchorage-independent growth capacity, than the cancer cells of adenocarcinoma (Usuda et al. 1994; Iyoda et al. 2004; Gudermann and Roelle 2006; Travis 2010). Thus, exogenous stromal factors produced by TAMs and Tregs may not have as much influence on the malignant behavior of HGNEC, compared with their effect on NSCLC.

The prognostic value of podoplanin-positive CAFs has been reported for various organs: as a predictor of an unfavorable prognosis in breast (Pula et al. 2011; Schoppmann et al. 2012) and cervical cancer, (Carvalho et al. 2010) and as a predictor of a favorable prognosis in colorectal cancer (Liang et al. 2005). The current study clearly shows that the presence of podoplanin-positive CAFs was a predictor of a favorable prognosis for both SCLC and LCNEC. Considering these results, HGNEC with podoplanin-positive CAFs may have a low malignant potential.

We previously reported that the expression of podoplanin in CAFs was a predictor of an unfavorable prognosis in patients with lung adenocarcinoma and squamous cell carcinoma (Kawase et al. 2008; Ito et al. 2012a; Ono et al. 2013), and the podoplanin expressed on CAFs is functionally responsible for tumor progression (Hoshino et al. 2011). In this sense, the function of podoplanin-positive CAFs on tumor cells was contradictory between lung adenocarcinoma and HGNEC. One possible explanation is that the signaling pathway through the ligand(s) for podoplanin on HGNEC differs from that for adenocarcinoma. We recently found that enhanced RhoA activity in fibroblasts expressing podoplanin may be one of the mechanisms resulting in the promotion of tumor formation, suggesting that biomechanical remodeling of the microenvironment by stromal fibroblasts may play an important role in tumor progression (Ito et al. 2012b). Signals that are transferred to cancer cells by CAFs have different effects on survival, invasion, and/or growth according to the kind of cancer cells as a result of ligand binding or extracellular matrix remodeling. Further study is needed to clarify the molecular mechanisms of podoplanin-positive CAFs in lung HGNEC, which would support the validity for a novel risk classification of patients and a basis for more effective treatment strategies for HGNEC.

A major drawback of this study is that the number of patients was relatively small. Future studies are required to confirm the prognostic significance of podoplanin-positive CAFs in validation populations using a multi-center trial.

In conclusion, the current study reported that podoplanin-positive CAFs had prognostic value in both SCLC and LCNEC. Our results imply that podoplanin expression reflects a tumor-inhibitory phenotype of CAFs in HGNEC. Although the exact mechanisms responsible for this phenomenon are not fully understood, our results provide novel insights into the pathogenesis of a unique microenvironment of HGNEC as well as basic data for new treatment strategies for HGNEC.

**Acknowledgments** This work was supported by National Cancer Center Research and Development Fund (23-A-12 and 23-K-18), the Foundation for the Promotion of Cancer Research, 3rd-Term Comprehensive 10-Year Strategy for Cancer Control, Program for the Promotion of Fundamental Studies in Health Sciences of the National Institute of Biomedical Innovation, and JSPS KAKENHI (24659185).

**Conflict of interest** None.

## References

Asamura H, Kameya T, Matsuno Y, Noguchi M, Tada H, Ishikawa Y, Yokose T, Jiang SX, Inoue T, Nakagawa K, Tajima K, Nagai K (2006) Neuroendocrine neoplasms of the lung: a prognostic spectrum. J Clin Oncol Off J Am Soc Clin Oncol 24(1):70–76. doi:10.1200/JCO.2005.04.1202

Bhowmick NA, Neilson EG, Moses HL (2004) Stromal fibroblasts in cancer initiation and progression. Nature 432(7015):332–337. doi:10.1038/nature03096

Bremnes RM, Donnem T, Al-Saad S, Al-Shibli K, Andersen S, Sirera R, Camps C, Marinez I, Busund LT (2011) The role of tumor stroma in cancer progression and prognosis: emphasis on carcinoma-associated fibroblasts and non-small cell lung cancer. J Thorac Oncol Off Publ Int Assoc Study Lung Cancer 6(1):209–217. doi:10.1097/JTO.0b013e3181f8a1bd

Carvalho FM, Zaganelli FL, Almeida BGL, Goes JCS, Baracat EC, Carvalho JP (2010) Prognostic value of podoplanin expression in intratumoral stroma and neoplastic cells of uterine cervical carcinomas. Clinics 65(12):1279–1283. doi:10.1590/s1807-59322010001200009

Chen X, Oppenheim JJ (2011) Resolving the identity myth: key markers of functional CD4 + FoxP3 + regulatory T cells. Int Immunopharmacol 11(10):1489–1496. doi:10.1016/j.intimp.2011.05.018

Dimitrakopoulos FI, Papadaki H, Antonacopoulou AG, Kottorou A, Gotsis AD, Scopa C, Kalofonos HP, Mouzaki A (2011) Association of FOXP3 expression with non-small cell lung cancer. Anticancer Res 31(5):1677–1683

Ding ZY, Zou XL, Wei YQ (2012) Cancer Microenvironment and Cancer Vaccine. Cancer Microenviron Off J Int Cancer Microenviron Soc. doi:10.1007/s12307-012-0107-x

Erler BS, Presby MM, Finch M, Hodges A, Horowitz K, Topilow AA, Matulewicz T (2011) CD117, Ki-67, and p53 predict survival in neuroendocrine carcinomas, but not within the subgroup of small cell lung carcinoma. Tumour Biol J Int Soc Oncodev Biol Med 32(1):107–111. doi:10.1007/s13277-010-0104-y

Gudermann T, Roelle S (2006) Calcium-dependent growth regulation of small cell lung cancer cells by neuropeptides. Endocr Relat Cancer 13(4):1069–1084. doi:10.1677/erc.1.01302

Hoshino A, Ishii G, Ito T, Aoyagi K, Ohtaki Y, Nagai K, Sasaki H, Ochiai A (2011) Podoplanin-positive fibroblasts enhance lung adenocarcinoma tumor formation: podoplanin in fibroblast functions for tumor progression. Cancer Res 71(14):4769–4779. doi:10.1158/0008-5472.CAN-10-3228

Igawa S, Watanabe R, Ito I, Murakami H, Takahashi T, Nakamura Y, Tsuya A, Kaira K, Naito T, Endo M, Yamamoto N, Kameya T (2010) Comparison of chemotherapy for unresectable pulmonary high-grade non-small cell neuroendocrine carcinoma and small-cell lung cancer. Lung Cancer 68(3):438–445. doi:10.1016/j.lungcan.2009.07.003

Ito M, Ishii G, Nagai K, Maeda R, Nakano Y, Ochiai A (2012a) Prognostic impact of cancer-associated stromal cells in stage I lung adenocarcinoma patients. Chest. doi:10.1378/chest.11-2458

Ito S, Ishii G, Hoshino A, Hashimoto H, Neri S, Kuwata T, Higashi M, Nagai K, Ochiai A (2012b) Tumor promoting effect of podoplanin-positive fibroblasts is mediated by enhanced RhoA activity. Biochem Biophys Res Commun 422(1):194–199. doi:10.1016/j.bbrc.2012.04.158

Iyoda A, Hiroshima K, Moriya Y, Mizobuchi T, Otsuji M, Sekine Y, Shibuya K, Iizasa T, Saitoh Y, Fujisawa T (2004) Pulmonary large cell neuroendocrine carcinoma demonstrates high proliferative activity. Ann Thorac Surg 77(6):1891–1895. doi:10.1016/j.athoracsur.2003.10.119 Discussion 1895

Iyoda A, Hiroshima K, Moriya Y, Takiguchi Y, Sekine Y, Shibuya K, Iizasa T, Kimura H, Nakatani Y, Fujisawa T (2006) Prospective study of adjuvant chemotherapy for pulmonary large cell neuroendocrine carcinoma. Ann Thorac Surg 82(5):1802–1807. doi:10.1016/j.athoracsur.2006.05.109

Karagoz B, Bilgi O, Gumus M, Erikci AA, Sayan O, Turken O, Kandemir EG, Ozturk A, Yaylaci M (2010) CD8 + CD28- cells and CD4 + CD25 + regulatory T cells in the peripheral blood of advanced stage lung cancer patients. Med Oncol 27(1):29–33. doi:10.1007/s12032-008-9165-9

Kawase A, Ishii G, Nagai K, Ito T, Nagano T, Murata Y, Hishida T, Nishimura M, Yoshida J, Suzuki K, Ochiai A (2008) Podoplanin expression by cancer associated fibroblasts predicts poor prognosis of lung adenocarcinoma. IJC Int J cancer 123(5):1053–1059. doi:10.1002/ijc.23611

Komohara Y, Hasita H, Ohnishi K, Fujiwara Y, Suzu S, Eto M, Takeya M (2011) Macrophage infiltration and its prognostic relevance in clear cell renal cell carcinoma. Cancer Sci 102(7):1424–1431. doi:10.1111/j.1349-7006.2011.01945.x

Koyama K, Kagamu H, Miura S, Hiura T, Miyabayashi T, Itoh R, Kuriyama H, Tanaka H, Tanaka J, Yoshizawa H, Nakata K, Gejyo F (2008) Reciprocal CD4 + T-cell balance of effector CD62Llow CD4 + and CD62LhighCD25 + CD4 + regulatory T cells in small cell lung cancer reflects disease stage. Clin Cancer Res Off J Am Assoc Cancer Res 14(21):6770–6779. doi:10.1158/1078-0432.CCR-08-1156

Kurahara H, Shinchi H, Mataki Y, Maemura K, Noma H, Kubo F, Sakoda M, Ueno S, Natsugoe S, Takao S (2011) Significance of M2-polarized tumor-associated macrophage in pancreatic cancer. J Surg Res 167(2):e211–e219. doi:10.1016/j.jss.2009.05.026

Liang P, Hong JW, Ubukata H, Liu G, Katano M, Motohashi G, Kasuga T, Watanabe Y, Nakada I, Tabuchi T (2005) Myofibroblasts correlate with lymphatic microvessel density and lymph node metastasis in early-stage invasive colorectal carcinoma. Anticancer Res 25(4):2705–2712

Ohtaki Y, Ishii G, Nagai K, Ashimine S, Kuwata T, Hishida T, Nishimura M, Yoshida J, Takeyoshi I, Ochiai A (2010) Stromal macrophage expressing CD204 is associated with tumor aggressiveness in lung adenocarcinoma. J Thorac Oncol Off Publ Int Assoc Study Lung Cancer 5(10):1507–1515. doi:10.1097/JTO.0b013e3181eba692

Ono S, Ishii G, Nagai K, Takuwa T, Yoshida J, Nishimura M, Hishida T, Aokage K, Fujii S, Ikeda N, Ochiai A (2013) Podoplanin-positive cancer-associated fibroblasts could have prognostic value independent of cancer cell phenotype in stage I lung squamous cell carcinoma: usefulness of combining analysis of both cancer cell phenotype and cancer-associated fibroblast phenotype. Chest 143(4):963–970. doi:10.1378/chest.12-0913

Petersen RP, Campa MJ, Sperlazza J, Conlon D, Joshi MB, Harpole DH Jr, Patz EF Jr (2006) Tumor infiltrating Foxp3 + regulatory T-cells are associated with recurrence in pathologic stage I NSCLC patients. Cancer 107(12):2866–2872. doi:10.1002/cncr.22282

Pollard JW (2004) Tumour-educated macrophages promote tumour progression and metastasis. Nat Rev Cancer 4(1):71–78. doi:10.1038/nrc1256

Pula B, Jethon A, Piotrowska A, Gomulkiewicz A, Owczarek T, Calik J, Wojnar A, Witkiewicz W, Rys J, Ugorski M, Dziegiel P, Podhorska-Okolow M (2011) Podoplanin expression by cancer-associated fibroblasts predicts poor outcome in invasive ductal breast carcinoma. Histopathology 59(6):1249–1260. doi:10.1111/j.1365-2559.2011.04060.x

Rossi G, Cavazza A, Marchioni A, Longo L, Migaldi M, Sartori G, Bigiani N, Schirosi L, Casali C, Morandi U, Facciolongo N, Maiorana A, Bavieri M, Fabbri LM, Brambilla E (2005) Role of chemotherapy and the receptor tyrosine kinases KIT, PDGFR-alpha, PDGFRbeta, and Met in large-cell neuroendocrine carcinoma of the lung. J Clin Oncol Off J Am Soc Clin Oncol 23(34):8774–8785. doi:10.1200/JCO.2005.02.8233

Ryuge S, Sato Y, Jiang SX, Wang G, Matsumoto T, Katono K, Inoue H, Iyoda A, Satoh Y, Yoshimura H, Masuda N (2012) Prognostic impact of nestin expression in resected large cell neuroendocrine carcinoma of the lung. Lung Cancer. doi:10.1016/j.lungcan.2012.03.025

Sarkaria IS, Iyoda A, Roh MS, Sica G, Kuk D, Sima CS, Pietanza MC, Park BJ, Travis WD, Rusch VW (2011) Neoadjuvant and adjuvant chemotherapy in resected pulmonary large cell neuroendocrine carcinomas: a single institution experience. Ann Thorac Surg 92(4):1180–1186. doi:10.1016/j.athoracsur.2011.05.027 Discussion 1186–1187

Schoppmann SF, Berghoff A, Dinhof C, Jakesz R, Gnant M, Dubsky P, Jesch B, Heinzl H, Birner P (2012) Podoplanin-expressing cancer-associated fibroblasts are associated with poor prognosis in invasive breast cancer. Breast Cancer Res Treat. doi:10.1007/s10549-012-1984-x

Shimizu K, Nakata M, Hirami Y, Yukawa T, Maeda A, Tanemoto K (2010) Tumor-infiltrating Foxp3 + regulatory T cells are correlated with cyclooxygenase-2 expression and are associated with recurrence in resected non-small cell lung cancer. J Thorac Oncol Off Publ Int Assoc Study of Lung Cancer 5(5):585–590. doi:10.1097/JTO.0b013e3181d60fd7

Sun JM, Ahn MJ, Ahn JS, Um SW, Kim H, Kim HK, Choi YS, Han J, Kim J, Kwon OJ, Shim YM, Park K (2012) Chemotherapy for pulmonary large cell neuroendocrine carcinoma: Similar to that for small cell lung cancer or non-small cell lung cancer? Lung Cancer. doi:10.1016/j.lungcan.2012.04.009

Tao H, Mimura Y, Aoe K, Kobayashi S, Yamamoto H, Matsuda E, Okabe K, Matsumoto T, Sugi K, Ueoka H (2012) Prognostic potential of FOXP3 expression in non-small cell lung cancer cells combined with tumor-infiltrating regulatory T cells. Lung Cancer 75(1):95–101. doi:10.1016/j.lungcan.2011.06.002

Travis WD (2010) Advances in neuroendocrine lung tumors. Ann Oncol Off J Eur Soc Med Oncol/ESMO 21(Suppl 7):65–71. doi:10.1093/annonc/mdq380

Travis WD, Linnoila RI, Tsokos MG, Hitchcock CL, Cutler GB Jr, Nieman L, Chrousos G, Pass H, Doppman J (1991) Neuroendocrine tumors of the lung with proposed criteria for large-cell neuroendocrine carcinoma. An ultrastructural, immunohistochemical, and flow cytometric study of 35 cases. Am J Surg Pathol 15(6):529–553

Usuda K, Saito Y, Sagawa M, Sato M, Kanma K, Takahashi S, Endo C, Chen Y, Sakurada A, Fujimura S (1994) Tumor doubling time and prognostic assessment of patients with primary lung cancer. Cancer 74(8):2239–2244

Usuda J, Ichinose S, Ishizumi T, Ohtani K, Inoue T, Saji H, Kakihana M, Kajiwara N, Uchida O, Nomura M, Ohira T, Ikeda N (2011a) Klotho predicts good clinical outcome in patients with limited-disease small cell lung cancer who received surgery. Lung Cancer 74(2):332–337. doi:10.1016/j.lungcan.2011.03.004

Usuda J, Ichinose S, Ishizumi T, Ohtani K, Inoue T, Saji H, Kakihana M, Kajiwara N, Uchida O, Nomura M, Tsutsui H, Ohira T, Ikeda N (2011b) Klotho is a novel biomarker for good survival in resected large cell neuroendocrine carcinoma of the lung. Lung Cancer 72(3):355–359. doi:10.1016/j.lungcan.2010.10.008

Wang W, Hodkinson P, McLaren F, Mackinnon A, Wallace W, Howie S, Sethi T (2012) Small cell lung cancer tumour cells induce regulatory T lymphocytes, and patient survival correlates negatively with FOXP3(+) cells in tumour infiltrate. IJC J Int Cancer. doi:10.1002/ijc.27613

Yamazaki S, Sekine I, Matsuno Y, Takei H, Yamamoto N, Kunitoh H, Ohe Y, Tamura T, Kodama T, Asamura H, Tsuchiya R, Saijo N (2005) Clinical responses of large cell neuroendocrine carcinoma of the lung to cisplatin-based chemotherapy. Lung Cancer 49(2):217–223. doi:10.1016/j.lungcan.2005.01.008

Cancer Science
The official journal of the Japanese Cancer Association

# Identification of a lung adenocarcinoma cell line with CCDC6-RET fusion gene and the effect of RET inhibitors *in vitro* and *in vivo*

Makito Suzuki,[1,2,11] Hideki Makinoshima,[1,11] Shingo Matsumoto,[1,3] Ayako Suzuki,[4] Sachiyo Mimaki,[1] Koutatsu Matsushima,[1,2] Kiyotaka Yoh,[3] Koichi Goto,[3] Yutaka Suzuki,[4] Genichiro Ishii,[5] Atsushi Ochiai,[5] Koji Tsuta,[6] Tatsuhiro Shibata,[7] Takashi Kohno,[8] Hiroyasu Esumi[9] and Katsuya Tsuchihara[1,2,10]

[1]Division of Translational Research, Research Center for Innovative Oncology, National Cancer Center Hospital East, Kashiwa, Chiba; [2]Department of Integrated Biosciences, Graduate School of Frontier Sciences, The University of Tokyo, Kashiwa, Chiba; [3]Division of Thoracic Oncology, National Cancer Center Hospital East, Kashiwa, Chiba; [4]Department of Medical Genome Sciences, Graduate School of Frontier Sciences, The University of Tokyo, Kashiwa, Chiba; [5]Division of Pathology, Research Center for Innovative Oncology, National Cancer Center Hospital East, Kashiwa, Chiba; [6]Division of Pathology and Clinical Laboratories, National Cancer Center Hospital, Tokyo; Divisions of [7]Cancer Genomics; [8]Genome Biology, National Cancer Center Research Institute, Tokyo; [9]National Cancer Center Hospital East, Kashiwa, Chiba, Japan

(Received December 4, 2012/Revised April 1, 2013/Accepted April 1, 2013/Accepted manuscript online April 11, 2013/Article first published online May 12, 2013)

**Rearrangements of the proto-oncogene *RET* are newly identified potential driver mutations in lung adenocarcinoma (LAD). However, the absence of cell lines harboring *RET* fusion genes has hampered the investigation of the biological relevance of RET and the development of RET-targeted therapy. Thus, we aimed to identify a *RET* fusion positive LAD cell line. Eleven LAD cell lines were screened for *RET* fusion transcripts by reverse transcription-polymerase chain reaction. The biological relevance of the *CCDC6-RET* gene products was assessed by cell growth, survival and phosphorylation of ERK1/2 and AKT with or without the suppression of RET expression using RNA interference. The efficacy of RET inhibitors was evaluated *in vitro* using a culture system and in an *in vivo* xenograft model. Expression of the *CCDC6-RET* fusion gene in LC-2/ad cells was demonstrated by the mRNA and protein levels, and the genomic break-point was confirmed by genomic DNA sequencing. Mutations in *KRAS* and *EGFR* were not observed in the LC-2/ad cells. CCDC6-RET was constitutively active, and the introduction of a siRNA targeting the *RET 3'* region decreased cell proliferation by downregulating RET and ERK1/2 phosphorylation. Moreover, treatment with RET-inhibitors, including vandetanib, reduced cell viability, which was accompanied by the downregulation of the AKT and ERK1/2 signaling pathways. Vandetanib exhibited anti-tumor effects in the xenograft model. Endogenously expressing CCDC6-RET contributed to cell growth. The inhibition of kinase activity could be an effective treatment strategy for LAD. LC-2/ad is a useful model for developing fusion RET-targeted therapy. (*Cancer Sci* 2013; 104: 896–903)**

Lung cancer is the most common cause of cancer death worldwide.[1] The identification of oncogenic driver genes is to select the increasing number of small molecule inhibitors targeting these gene products.[2,3] In particular, in lung adenocarcinoma (LAD), the most dominant histological subtype of lung cancer, the application of kinase inhibitors for cases with specific gene alterations has been successful, that is, gefitinib and erlotinib for *EGFR* mutation-positive cases and crizotinib for *ALK* fusion-positive cases.[4–7] Furthermore, accumulating evidence has demonstrated somatic mutations and rearrangements of potential oncogenes, including *BRAF*, *ERBB2* and *ROS1*, in LAD.[8–10]

*RET* is one of the newest LAD driver genes.[11–15] *RET* gene is located on chromosome 10 and encodes a receptor tyrosine kinase,[16,17] and the oncogenic potential of this gene product has been suggested in several tumors, including thyroid cancer.[18–20] Recently, five independent groups identified aberrant fusion genes, *KIF5B-RET* and *CCDC6-RET* in clinical samples of LAD.[11–15] Ectopically expressed RET fusion products afforded NIH3T3 cells with anchorage-independent growth and tumorigenicity in nude mice.[11,14] Furthermore, KIF5B-RET-expressing H1299 cells exhibited growth factor-independent growth.[11] These findings strongly suggest the oncogenic activity of RET fusion products and also suggest the potential therapeutic efficacy of multi-kinase inhibitor targeting of RET using the abovementioned cells. However, LAD-derived cell lines harboring *RET* fusion genes had not been identified. Recently, Matsubara *et al.*[21] screened LAD cell lines that were sensitive to a RET inhibitor vandetanib and found a *CCDC6-RET* fusion gene-harboring cell line, LC-2/ad.

We have independently screened cell lines established from Japanese LAD samples by RT-PCR and found that LC-2/ad cells expressed the *CCDC6-RET* fusion gene product. We further examined whether LC-2/ad cells depend on RET fusion-mediated signaling. In addition, the antitumor effect of RET inhibitors in LC-2/ad cells was evaluated *in vitro* and *in vivo*.

## Materials and Methods

Complete materials and methods were described in the supplementary information (Data S1. Materials and Methods).

**Purchased materials.** Cell lines were purchased from RIKEN Bio Resource Center, the Immuno-Biological Laboratories (Fujioka, Japan) and American Type Culture Collection. Procedures for western blotting was previously described.[22] Primary antibodies specific for RET and phospho-RET Tyr-905 were purchased from Epitomics (Burlingame, CA, USA) and Cell Signaling Technologies (Danvers, MA, USA), respectively. RET-targeting siRNA was purchased from Life Technologies (Carlsbad, CA, USA). Gefitinib, sunitinib malate and sorafenib were purchased from Santa Cruz Biotechnology (Dallas, TX, USA), Sigma-Aldrich (St. Louis, MO, USA) and Toronto Research Chemicals (Toronto, ON, Canada),

[10]To whom correspondence should be addressed.
E-mail: ktsuchih@east.ncc.go.jp
[11]These authors contributed equally to this work.


doi: 10.1111/cas.12175

respectively. Vandetanib, AZD6244 and BEZ235 were purchased from Selleck (Houston, TX, USA).

**Multiplex RT-PCR.** Reported *KIF5B/CCDC6-RET* fusion variants were detected by multiplex RT-PCR according to the procedures described elsewhere.[11,14]

**Genomic DNA sequencing.** LC-2/ad DNA was captured with custom hybridization probes targeting *CCDC6* intron 1 and *RET* whole gene (Agilent) followed by parallel sequencing on the MiSeq system (Illumina).

**Real-time RT-PCR.** Procedures for real-time RT-PCR was previously described.[22] The PCR primers used in the present study are shown in Table S1.

***In vivo* studies.** LC2/ad cells at $5.0 \times 10^6$ were subcutaneously inoculated to 8-week-old athymic nude mice (Clea Japan).[23] Vandetanib was administered once daily as a homogeneous suspension by oral gavage at a dosage of 50 mg/kg body weight.[24] The tumor volume was calculated as the product of a scaling factor ($\pi/6$) and the tumor length, width and height.[22] The study was approved by the Institutional Ethics Review Committee for animal experiments at the National Cancer Center.

**Immunohistochemical analysis.** The procedure for hematoxylin eosin staining and immunohistochemical (IHC) was previously described.[22,25]

**Microarray analysis.** Background information of clinical samples was described in a previous report.[26] The study was approved by the Institutional Review Boards of the National Cancer Center. Total RNA was analyzed using Affymetrix (Santa Clara, CA, USA) U133Plus2.0 arrays. The data were processed by the MAS5 algorithm, and the mean expression level of a total of 54 675 probes was adjusted to 1000 for each sample.

## Results

**Identification of the *CCDC6-RET* fusion gene in a Japanese LAD cell line.** To identify *RET* fusion-derived mRNA expression in human LAD cell lines, all reported *KIF5B-RET* and *CCDC6-RET* gene products were screened by multiplex RT-PCR in 11 cell lines derived from Japanese patients. LC-2/ad cells were found to express *CCDC6-RET* mRNA at significantly higher levels, whereas the other cell lines did not exhibit any fusion gene products (Fig. 1a). The expressed fusion *RET* product was sequenced, and an in-frame fusion of *CCDC6* exon 1 and *RET* exon 12, which was identical to the previously reported *CCDC6-RET* fusion products, was identified (Fig. 1b).[14] We then identified a breakpoint of chromosome 10 by retrieving genomic DNA fragments, including the entire *RET* gene and intron 1 of *CCDC6*, by target capture system followed by parallel sequencing. The identified break-point between *CCDC6* intron 1 and *RET* exon 11 was confirmed by Sanger sequencing (Fig. 1b). Quantitative RT-PCR revealed that the expression of 3′ end of *RET* was increased comparable to that of *CCDC6*, whereas the transcript level of the 5′ end of *RET* was significantly lower (Fig. 1c). Consistent with the amount of transcript, western blotting using an antibody recognizing the C-terminus of RET isoform 2 detected a 60-kDa specific band equivalent to

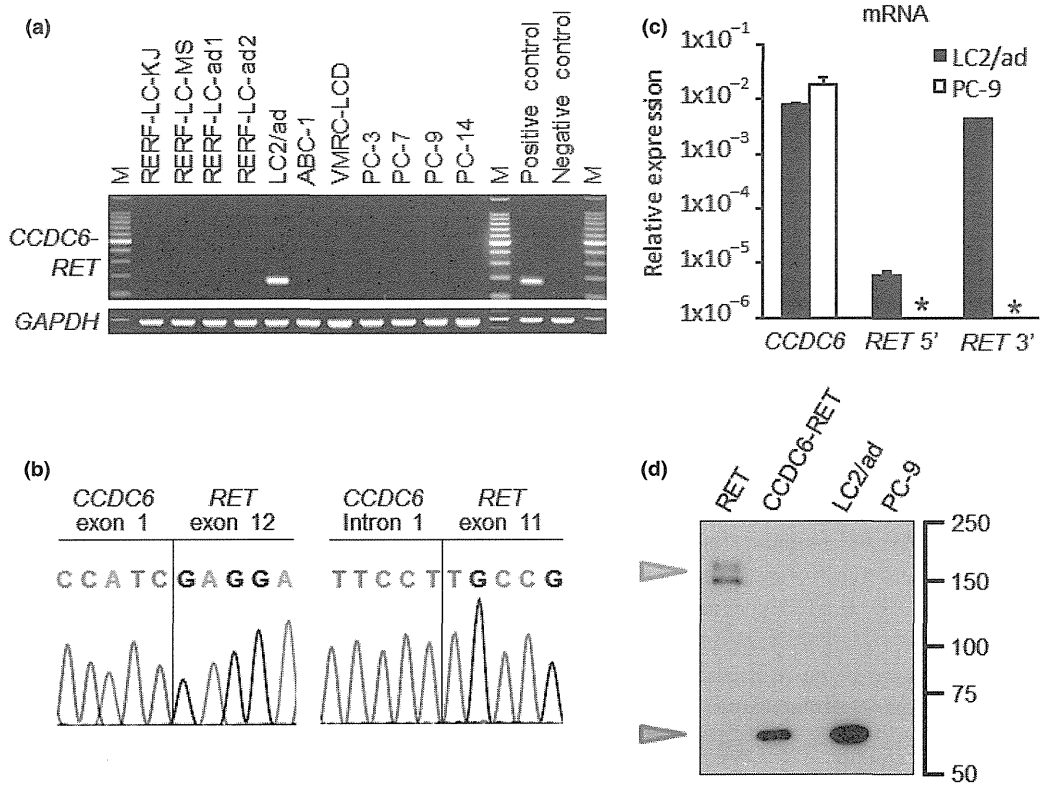


**Fig. 1.** Identification of the *CCDC6-RET* fusion gene. (a) Detection of *RET* fusion transcripts in lung adenocarcinoma (LAD) cell lines by multiplex reverse transcription-polymerase chain reaction (RT-PCR). (b) Sanger sequencing around the fusion point of the cDNA (left) and the breakpoint of the genomic DNA (right) of *CCDC6-RET* in LC-2/ad cells. (c) 3′ region-specific expression of *RET* mRNA in LC-2/ad cells. The 5′ or 3′ region of *RET* and *CCDC6* cDNA level was normalized to glyceraldehyde 3-phosphate dehydrogenase (*GAPDH*) expression. The data are shown as the mean ± standard deviation (SD) ($n = 3$). Asterisks indicate that mRNA expression were below the level of detection. (d) Specific expression of the CCDC6-RET fusion protein. Whole-cell lysates of LC2/ad and PC-9 cells and HEK293 cells transfected with wild-type RET (RET) or CCDC6-RET expression plasmids were subjected to western blot analysis to detect RET protein isoform 2. The LC-2/ad cells showed an approximately 60-kDa (red arrowhead) but not 170-kDa (blue arrowhead) band.

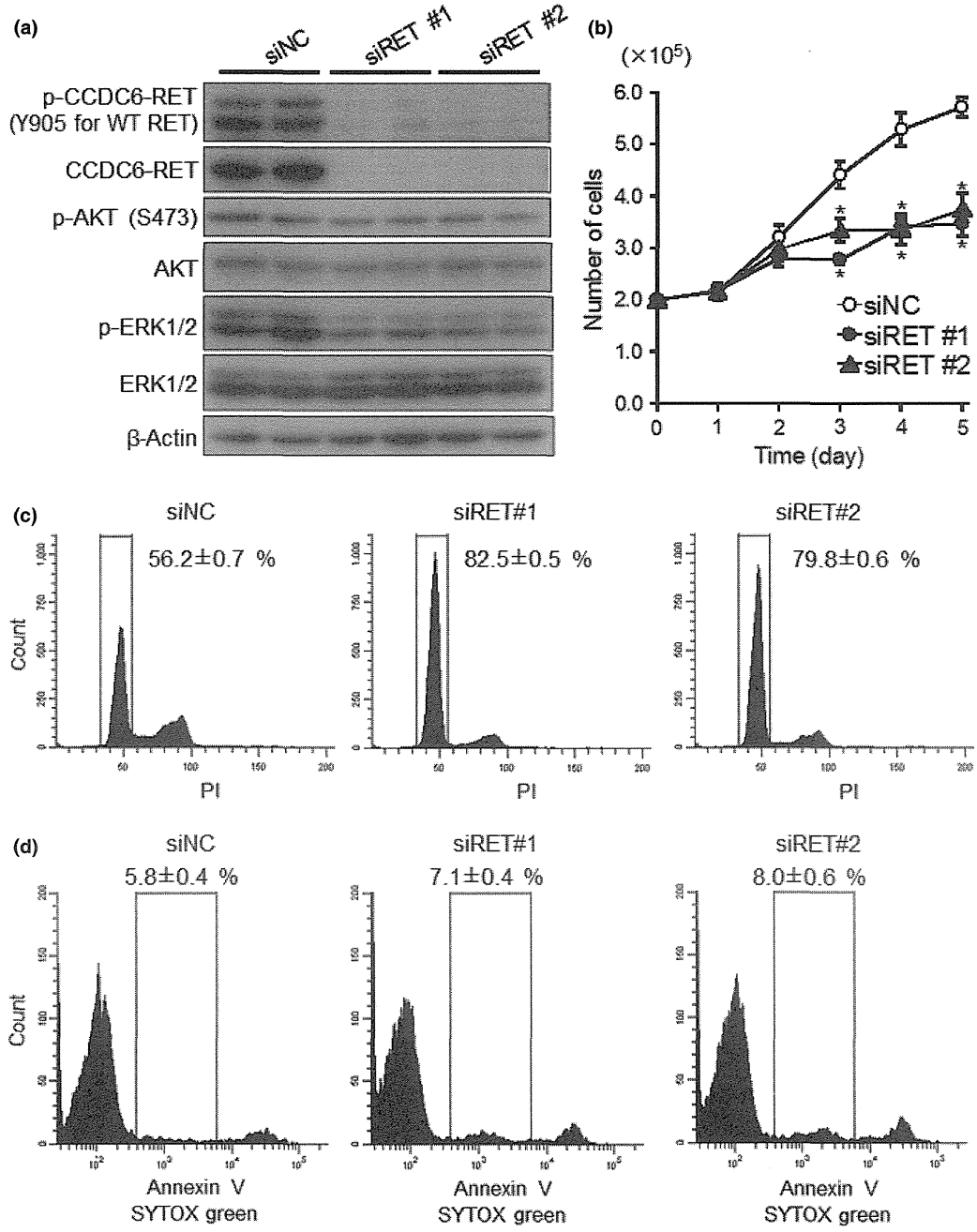


**Fig. 2.** Suppression of CCDC-RET expression by siRNA in LC-2/ad cells. (a) Western blot analysis of siRET-treated LC-2/ad cells. The siRNA transfected cell lysates were applied to the western blotting. (b) Involvement of RET suppression in cell growth inhibition. LC-2/ad cells transfected with siRNAs were incubated for the indicated times. The data are shown as the mean ± standard deviation (SD) ($n$ = 4). *$P$ < 0.01 (Student's $t$-test). (c,d) The DNA ploidy (c) and Annexin V-positive population (d) of siRET-transfected LC-2/ad cells. After 72 h of siRNA transfection, the cells were subjected to DNA ploidy analysis and Annexin V staining. The data are shown as the mean ± SD ($n$ = 4).

the estimated size of the fusion protein composed of 503 amino acids (GeneBank BAM36435), whereas no significant signal was detected that approximated the size of wild-type RET, 170-kDa (Fig. 1d).[11] Taken together, we concluded that LC-2/ad cells express *CCDC6-RET* fusion gene products. *KRAS* exon 2 and *EGFR* exon 19 and 21 were examined by Sanger sequencing, but no obvious mutation was confirmed (Fig. S1).

**CCDC6-RET-dependent ERK1/2 phosphorylation and the proliferation of LC-2/ad cells.** We suppressed *RET* expression by RNAi to characterize the function of CCDC6-RET in LC-2/ad cells. For avoiding off-target siRNA effects, two different sequences of siRNA directed against the 3′ region of *RET* (siRET#1 and #2) and a nontargeting siRNA (siNC) were used. When compared to siNC, a significant reduction in mRNA expression was observed by quantitative RT-PCR detecting the 3′ end of the *RET* mRNA: 66.5% for siRET#1 and 94.2% for siRET#2 (Fig. S2). Western blot analyses also revealed significant decreases in the expression of CCDC6-RET protein (60-kDa) upon the introduction of siRET#1 and #2 compared to the control siNC in the LC-2/ad cells


doi: 10.1111/cas.12175

(Fig. 2a). To examine whether the downstream signaling pathway was altered by the introduction of siRNA, the phosphorylation of ERK1/2 and AKT was examined. The phospho-ERK1/2 signal was significantly decreased by the suppression of CCDC6-RET expression, whereas the decrease of AKT phosphorylation was marginal (Fig. 2a). The involvement of RET fusion in LC-2/ad cell proliferation was then examined. The number of live CCDC6-RET-suppressed cells decreased throughout the experiment, and the difference became significant at day 3 and thereafter (Fig. 2b). To address the growth suppression further, the cell cycle of the siRNA-treated cells were assessed by the DNA ploidy pattern. The LC-2/ad cells treated with siRET exhibited significant increases in the percent of cells arrested in the G1 phase relative to the cells treated with siNC (Fig. 2c). However, the apoptotic cells, as assessed by Annexin V positivity, was not significantly increased by the suppression of RET expression (Fig. 2d).

**RET-dependent transcriptome profile in LC-2/ad cell.** To characterize the transcriptome profile, which is regulated by CCDC6-RET and its downstream signaling pathway, siRET#2 and siNC treated LC-2/ad cells were subjected to genome-wide expression profiling using Affymetrix U133Plus2.0 arrays. A total of 243 genes, evaluated with 285 probes were selected as those preferentially suppressed by less than half in siRET-treated cells.As well, 566 genes with 661 probes were expressed more than twice in siRET-treated cells (Table S2 and Fig. S3). The *RET* gene itself (probe ID = 211421_s_at) showed the highest fold-difference of 19.6 between siNC- and siRET#2-treated cells. Following *RET*, previously identified Gene Ontology-annotated Ras-MAPK downstream genes like *DUSP6* was preferentially suppressed in the siRET-treated cells. In addition, cell cycle regulation-related genes like *EREG, CDC6, MCM10, MAD2L1, CHEK1* and *PLK4* were expressed <0.5-fold in siRET-treated cells (Table 1).

*RET* fusion gene screening of 300 consecutive surgically resected LAD samples identified one case of *CCDC6-RET* expressing LAD by RT-PCR and break-apart FISH (Tsuta *et al.*, 2012, unpublished data). We checked the expression level of potential CCDC6-RET-driven genes identified above in the clinical sample. Among 285 preferentially expressed probes, 81 probes were also upregulated more than twofold in the *CCDC6-RET* positive LAD tissue compared to the surrounding non-cancerous tissue (Table 1 and Table S2).

**RET inhibitor-induced cell cycle arrest and apoptosis in LC-2/ad cells.** The phosphorylation status of the tyrosine 905 residue of RET isoforms 2 and 4 was high in the LC-2/ad cells, regardless of the presence or absence of serum in the culture medium, whereas the total amount of RET isoform 2 was not significantly altered. Similarly, the phosphorylation status of AKT and ERK1/2 was high under serum-starved conditions, and the enhanced phosphorylation of these molecules was slight with serum stimulation, suggesting that the fusion RET kinase was constitutively active and activated its downstream signaling pathways (Fig. 3a).

Next, the effects of kinase inhibitors, which inhibit spectrum including RET were applied to evaluate their effects on the signaling pathways in the LC-2/ad cells. We treated the cells with RET inhibitors vandetanib, sunitinib and sorafenib at a final concentration of 10 μM, which was 10–30 times higher than the *in vitro* half maximal inhibitory concentration ($IC_{50}$) for RET kinase activity of each compound. Gefitinib, another small molecule inhibitor targeting EGFR but not RET,[13] was also examined. All the inhibitors except gefitinib significantly suppressed the phosphorylation of RET, AKT and ERK1/2. Although vandetanib, sunitinib and sorafenib equivalently suppressed RET phosphorylation, vandetanib most significantly suppressed the phosphorylation of ERK1/2 (Fig. 3a). The inhibitory effect of vandetanib on RET, AKT and ERK1/2 phosphorylation exhibited concentration dependency (Fig. 3b). Gefitinib significantly suppressed EGFR phosphorylation while total EGFR protein level was not altered. Meanwhile, gefitinib did not alter the phosphorylation status of AKT and ERK1/2 (Fig. 3a). Meanwhile, vandetanib suppressed EGFR as well as AKT and ERK1/2 in *EGFR*-mutant PC-9 cells (Fig. S4).

We further examined the effect of the above inhibitors on the growth of the LC-2/ad cells using the WST-8 assay. Consistent with the effects of the inhibitors on the RET signaling pathway, vandetanib suppressed cell growth most significantly ($IC_{50}$ = 0.32 μM), followed by sunitinib and sorafenib, whereas gefitinib only exhibited an apparent suppression at its highest dose (Fig. 3c). However, the effects of these inhibitors on *KRAS*-mutant A549 cells were much lower (Fig. S5). Gefitinib and vandetanib, both of which inhibit EGFR, suppressed *EGFR*-mutant PC-9 cells, whereas sunitinib and sorafenib had less effect (Fig. S5). Evaluating the number of live cells by trypan blue staining under the treatment of several doses of

**Table 1. Up- or downregulated genes associated with mitogen-activated protein kinase (MAPK) cascade or cell cycle**

| Gene symbol | Probe set ID | siNC/siRET | Tumor/Non-tumor |
|---|---|---|---|
| Upregulated | | | |
| *RET* | 211421_s_at | 19.63 | 19.52 |
| | 205879_x_at | 3.76 | 5.03 |
| | 215771_x_at | 2.37 | 4.72 |
| *DUSP6* | 208892_s_at | 4.45 | 5.22 |
| | 208893_s_at | 4.17 | 6.34 |
| | 208891_at | 4.17 | 3.56 |
| *EREG* | 1569583_at | 3.68 | 1.60 |
| | 205767_at | 2.93 | 5.69 |
| *CDC6* | 203967_at | 2.42 | 4.82 |
| | 203968_s_at | 1.95 | 5.32 |
| *MCM10* | 220651_s_at | 2.30 | 4.83 |
| | 223570_at | 1.72 | 1.71 |
| *MAD2L1* | 203362_s_at | 2.28 | 5.91 |
| | 1554768_a_at | 1.91 | 4.34 |
| *CHEK1* | 205394_at | 2.17 | 9.03 |
| | 205393_s_at | 2.14 | 6.87 |
| *PLK4* | 204886_at | 2.07 | 4.38 |
| | 204887_s_at | 1.56 | 4.08 |
| Downregulated | | | |
| *MEF2C* | 209200_at | 0.21 | 0.46 |
| | 209199_s_at | 0.26 | 0.65 |
| *GAB1* | 214987_at | 0.23 | 0.42 |
| | 229114_at | 0.53 | 0.65 |
| | 225998_at | 0.62 | 0.68 |
| | 226002_at | 0.64 | 0.76 |
| *CDKN1C* | 216894_x_at | 0.26 | 0.41 |
| | 213348_at | 0.32 | 0.23 |
| | 213183_s_at | 0.35 | 0.30 |
| | 219534_x_at | 0.42 | 0.27 |
| | 213182_x_at | 0.44 | 0.21 |
| *PTEN* | 233314_at | 0.33 | 0.27 |
| | 225363_at | 0.77 | 0.47 |
| *TIMP2* | 231579_s_at | 0.34 | 0.33 |
| | 224560_at | 0.37 | 0.27 |
| *ID2* | 201566_x_at | 0.35 | 0.31 |
| | 201565_s_at | 0.40 | 0.39 |
| | 213931_at | 0.52 | 0.31 |
| *CCNL2* | 232274_at | 0.35 | 0.42 |
| | 222999_s_at | 0.79 | 0.52 |
| *RPS6KA2* | 212912_at | 0.41 | 0.34 |
| | 204906_at | 0.59 | 0.49 |

vandetanib suggested a dose-dependent suppression in the LC-2/ad cells. Furthermore, the number of cells treated with 0.5 and 1.0 μM vandetanib was apparently reduced to less than the starting amount, strongly suggesting that vandetanib induced both cell death and the suppression of cell proliferation (Fig. 3d). An assessment of the DNA ploidy revealed that vandetanib arrested the cell cycle in G1 phase in a dose-dependent manner (Fig. 3e), and an increased concentration of vandetanib induced an Annexin V-positive apoptotic cell population (Fig. 3f). The proapoptotic effect of vandetanib was confirmed by the detection of cleaved caspase-3 by western blotting (Fig. 3b). Meanwhile, 1.0 μM sunitinib and sorafenib induced cell cycle arrest but induction of apoptosis was marginal (Figs S6 and S7).

To further evaluate the contribution of Ras-ERK and AKT axes to cell survival, LC-2/ad cells were treated with MEK1/2 inhibitor AZD6244 or PI3K/mTOR inhibitor BEZ235. Cytotoxic effect of AKT-inhibiting BEZ235 was more than that of ERK-inhibiting AZD6244. However, both inhibitors did not completely reduce the cell survival even their maximal dose (Figs S8 and S9).

**Anti-tumor effect of vandetanib in an LC-2/ad xenograft model.** Subcutaneously transplanted LC-2/ad tumors exhibited typical adenocarcinoma morphology. These tumors were positive for SFTPA, Napsin A and carcinoembryonic antigen (CEA) but thyroid marker thyroglobulin negative using immunohistochemistry (IHC). Furthermore, using an antibody cross-reacting with both human and mouse RET protein, IHC revealed that RET was highly expressed specifically in the tumor cells but not in the interstitial cells (Fig. 4a). The overexpression of RET in these tumors was confirmed using quantitative RT-PCR and Western blotting. Similar to the results from cultured LC-2/ad cells, much more mRNA of the 3′ end of *RET* was detected than that of the 5′ end (Fig. 4b), and a specific band equivalent to the size of the CCDC6-RET fusion protein was detected (Fig. 4c). Vandetanib (50 mg/kg) was orally administrated to the mice harboring the LC-2/ad xenograft, and the daily administration of vandetanib significantly reduced the tumor size. Although the tumors were diminished at day 14 of the treatment, the body weight of the treated mice was not significantly reduced (Fig. 4d and Fig. S10). Sorafenib (30 mg/kg) and sunitinib (40 mg/kg) did not reduce the body weight, either (Fig. S10). Sorafenib reduced but not diminished the tumors at day14. Anti-tumor effect of sunitinib was not significant (Fig. S11).

## Discussion

Previous reports suggest that the incidence of *RET*-fusion-positive cases in LAD is 1–2% and that these cases are concentrated in the *EGFR* mutation-, *KRAS* mutation-, and *ALK*-fusion-negative population.[10,27] To identify cell lines expressing endogenous *RET*-fusion genes, we selected 11 cell lines that were derived from pathologically identified Japanese LAD cases. Among them, activating EGFR mutations have been reported in PC-3 and PC-9 cells.[28] However, the mutation status of known driver genes of other cell lines was not well investigated. The LC-2/ad cells were originally derived from pleural effusion of LAD in a patient who had received combined chemotherapy (endoxan, Adriamycin, Cisplatin and mitomycin C)[23]; the cancer was diagnosed by cytological examination of the patient's sputum and pleural effusion. The original report indicated that the LC-2/ad cells were positive for an adenocarcinoma marker, cytokeratin 18.[23] In addition, we detected surfactant protein, an aspartate proteinase, Napsin A, and CEA expression in the xenograft tumor (Fig. 4a). These findings support the origin of LC-2/ad as lung adenocarcinoma. The modal chromosome number described in the original report was 53–56, though an apparent translocation between the chromosomes was not reported, consistent with the fact that the inversion of chromosome 10 was not obvious in the conventional chromosome counts.

The Sanger sequencing in this study and the whole-transcriptome sequencing (Tsuchihara, 2012, unpublished data) revealed no driver mutations of *KRAS*, *EGFR* and known genes other than the *CCDC6-RET* fusion in the LC-2/ad cells, highly suggesting that the CCDC6-RET fusion protein plays pivotal roles in the proliferation of these cells. The autophosphorylation of CCDC6-RET was clearly observed in a serum-independent manner, accompanied with a constitutive elevation of ERK1/2 phosphorylation. The suppression of CCDC6-RET expression induced a decrease in ERK1/2 phosphorylation, accompanied with a decrease in the expression of the genes that regulate the cell cycle. As a result, the CCDC6-RET-suppressed cells exhibited significant growth retardation.

Recently, a Japanese group independently reported the CCDC6-RET fusion in LC2/ad cells.[21] However, the efficacy of RET inhibitors to the RET and downstream pathways and *in vivo* anti-tumor effects have been partially described.[21] Vandetanib, sorafenib and sunitinib suppress the activities of multiple kinases, including RET, and have been approved for several cancers.[29–31] In *in vitro* analyses, these compounds effectively suppressed the phosphorylation of CCDC6-RET and suppressed proliferation and induced death in LC-2/ad cells. It should be noted that the $IC_{50}$ value for the growth suppression of these compounds was equivalent to the dose suggested in a previous study using culture cells expressing ectopic *KIF5B-RET* cDNA.[13] These effects were most likely dependent on RET inhibition. Sunitinib and sorafenib did not affect PC-9 and A549 cells, which have activating mutations of *EGFR* and *KRAS*, respectively. Vandetanib presumably suppressed the growth of PC-9 cells, as EGFR is included in its inhibitory spectrum. Meanwhile, gefitinib, which targets EGFR but not RET, did not significantly suppress the growth of LC-2/ad cells. Interestingly, gefitinib did not alter the phosphorylation of AKT and ERK1/2 in LC-2/ad cells albeit equivalently suppressing EGFR phosphorylation as vandetanib. Although precise molecular mechanisms should be further examined, LC-2/ad cells might not depend on EGFR for transducing downstream signaling.

Vandetanib exhibited apparent anti-tumor effects in the xenograft model in this study. Recently, efficacy of vandetanib on thyroid cancer cells harboring *RET*-fusion gene was also reported.[32] These findings strongly suggest that RET inhibition is a plausible therapeutic strategy for RET-fusion-positive tumors.

We noticed a discrepancy between the effects of RNA interference and inhibitor treatment on RET. Though RET suppression/inhibition equivalently reduced the level of phosphorylated RET and induced cell cycle arrest, obvious apoptosis was not found in the cells treated with siRNA. A possible explanation is that CCDC6-RET is mainly involved in the RAS-ERK pathway to regulate cell proliferation, whereas the anti-apoptotic signaling pathway mediated by AKT could be regulated by other signaling molecules inhibited by the multi-kinase inhibitors. A recent study using a Drosophila *in vivo* screening system suggested that the antitumor effects and toxicity of RET inhibitors were dependent on the profile of the "off-target" inhibition of multiple kinases in addition to the specific inhibition of RET.[33] Further investigation elucidating the molecules and signaling pathways relevant to the cytotoxic effect of vandetanib in LC-2/ad cells is anticipated.

Whether LC-2/ad-based models adequately represent clinical *RET* fusion-positive LAD cases is another challenging question. Takeuchi stated that clinically identified *CCDC6-RET*-positive LAD exhibited a histologically cribriform pattern.[14]


doi: 10.1111/cas.12175

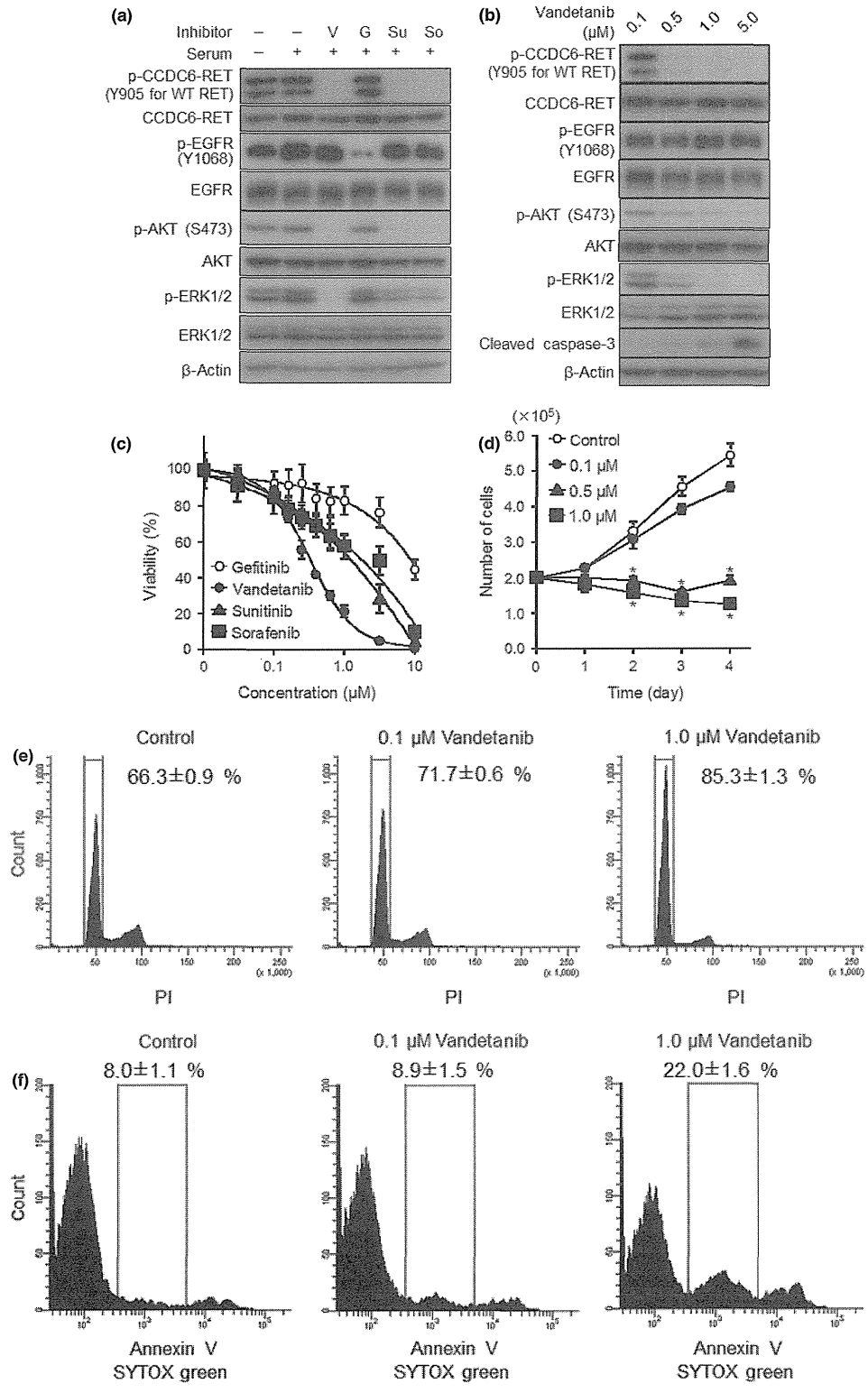


**Fig. 3.** Effect of RET inhibitors on LC-2/ad cells. (a) Western blot analysis of inhibitor-treated cells. The cells were incubated under serum-starved conditions for 22 h and treated with 1 μM of inhibitor or dimethylsulfoxide (DMSO) for 2 h. Prior to cell lysis, the cells were treated with 10% fetal bovine serum (FBS) for 10 min. Whole-cell lysates were subjected to western blot analysis to detect the indicated proteins. G, gefitinib; So, sorafenib; Su, sunitinib; V, vandetanib. (b) Dose-dependent effect of vandetanib. Cells were treated with the indicated concentration of vandetanib for 12 h, and western blotting was used to detect the indicated proteins. (c) WST-8 assay with kinase inhibitors. Cells were treated with the indicated inhibitors for 72 h, and the viability was assessed using the WST-8 assay. The data are shown as the mean ± standard deviation (SD) ($n$ = 6). (d) Effect of vandetanib for growth inhibition. Cells were treated with vandetanib and incubated for the indicated time. The data are shown as the mean ± SD ($n$ = 3). *$P$ < 0.01 (Student's $t$ test). (e,f) DNA ploidy (e) and Annexin V-positive population (f) of the cells treated with vandetanib for 48 h. The data are shown as the mean ± SD ($n$ = 4).

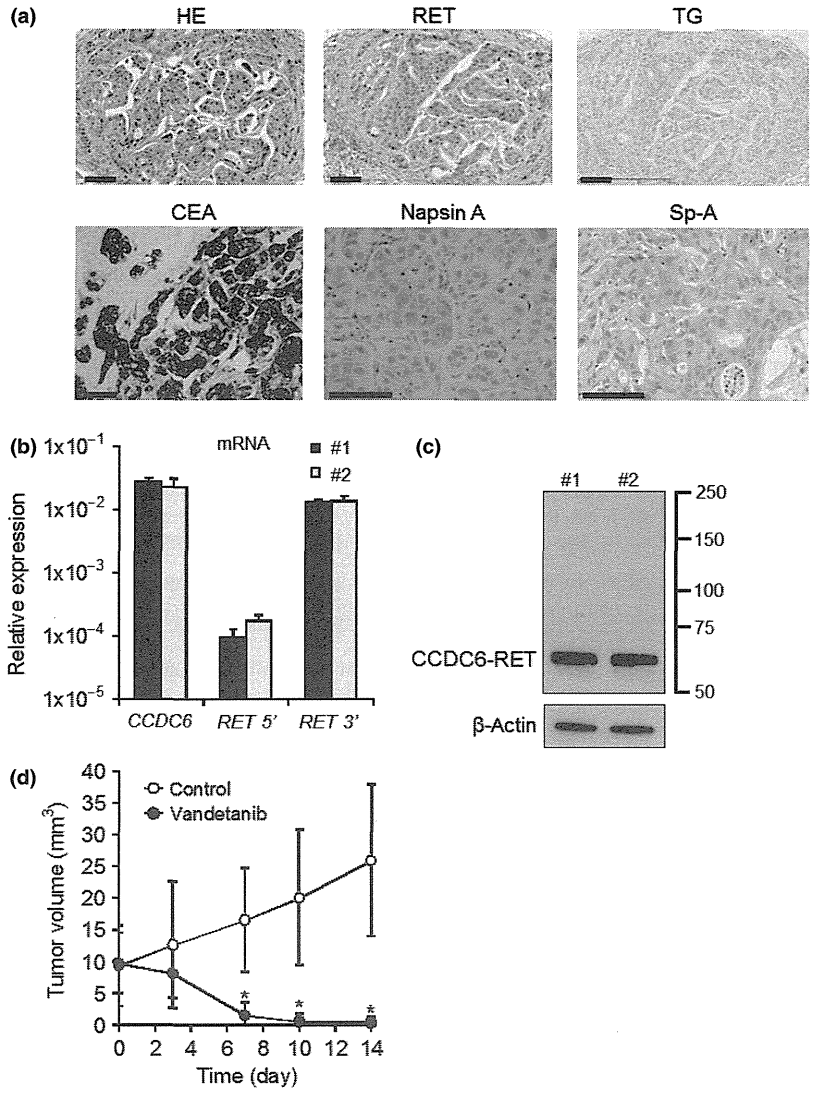


**Fig. 4.** Characterization of the LC-2/ad xenograft and anti-tumor effects of vandetanib. (a) Histological features of the xenograft. Hematoxylin and eosin staining and immunohistochemical staining with the indicated antibodies. Scale bars were 100 μm. Hematoxylin eosin (HE), RET, thyroglobulin (TG) and carcinoembryonic antigen (CEA) (×20); Napsin A and Sp-A (×40). (b) 3′ region-specific expression of *RET* mRNA in the xenograft. Total RNA extracted from tumors was subjected to real-time reverse transcription-polymerase chain reaction (RT-PCR) analysis with the primer sets designed for the 5′ or 3′ region of the *RET* and *CCDC6* cDNA. The data are shown as the mean ± standard deviation (SD) ($n = 3$). (c) Expression of the CCDC6-RET protein in mice xenografts. Whole-cell lysates of tumors were subjected to western blot analysis. (d) Anti-tumor effect of vandetanib *in vivo*. Vandetanib was administered once a day at a dosage of 50 mg/kg. The data are shown as the mean ± SD ($n = 9$). *$P < 0.01$ (control *vs* sorafenib; Student's *t* test).

Because the cribriform structure was presumably developed from normal alveolar architecture, this specific morphology was not observed in the subcutaneously transplanted LC-2/ad tumors. We assume that the comparison of the transcriptome profile between the LC-2/ad cells and clinically identified LAD tissue samples may provide clues. Approximately one-third of the genes suppressed by RNA interference directed at *RET* overlapped with the genes preferentially expressed in the clinical tumor sample. Because we have had only one example of paired data, it is difficult to estimate the similarity between the cell line and clinical samples. However, the above overlap appears promising, and we will continue to screen both cell lines and clinical samples to accumulate comprehensive data.

In this study, the screening of Japanese LAD cell lines was effective for the identification of *RET* fusion-positive cancer cells, representing a clinically rare subpopulation. LC-2/ad cells might be useful in the development of RET-targeted therapies, that is, new compound screening, clarifying the pharmacological mechanisms and investigating the mechanisms for acquired resistance.

## Acknowledgments

We thank Drs Hiroki Sasaki and Kazuhiko Aoyagi and the National Cancer Center Research Core Facility for the microarray analyses. The Core Facility was supported by National Cancer Center Research and Development Fund (23-A-7). This work was supported by National Cancer Center Research and Development Fund (23-A-8, 15, 24-A-1) and JSPS KAKENHI Grant number 24300345.

## Disclosure Statement

The authors have no conflict of interest.

## References

1 Jemal A, Bray F, Center MM, Ferlay J, Ward E, Forman D. Global cancer statistics. *CA Cancer J Clin* 2011; **61**: 69–90.
2 Pao W, Girard N. New driver mutations in non-small-cell lung cancer. *Lancet Oncol* 2011; **12**: 175–80.
3 Pao W, Chmielecki J. Rational, biologically based treatment of EGFR-mutant non-small-cell lung cancer. *Nat Rev Cancer* 2010; **10**: 760–74.



doi: 10.1111/cas.12175

4 Kwak EL, Bang YJ, Camidge DR *et al.* Anaplastic lymphoma kinase inhibition in non-small-cell lung cancer. *N Engl J Med* 2010; **363**: 1693–703.
5 Lynch TJ, Bell DW, Sordella R *et al.* Activating mutations in the epidermal growth factor receptor underlying responsiveness of non-small-cell lung cancer to gefitinib. *N Engl J Med* 2004; **350**: 2129–39.
6 Paez JG, Janne PA, Lee JC *et al.* EGFR mutations in lung cancer: correlation with clinical response to gefitinib therapy. *Science* 2004; **304**: 1497–500.
7 Tsao MS, Sakurada A, Cutz JC *et al.* Erlotinib in lung cancer – molecular and clinical predictors of outcome. *N Engl J Med* 2005; **353**: 133–44.
8 Govindan R, Ding L, Griffith M *et al.* Genomic landscape of non-small cell lung cancer in smokers and never-smokers. *Cell* 2012; **150**: 1121–34.
9 Imielinski M, Berger AH, Hammerman PS *et al.* Mapping the hallmarks of lung adenocarcinoma with massively parallel sequencing. *Cell* 2012; **150**: 1107–20.
10 Seo JS, Ju YS, Lee WC *et al.* The transcriptional landscape and mutational profile of lung adenocarcinoma. *Genome Res* 2012; **22**: 2109–19.
11 Kohno T, Ichikawa H, Totoki Y *et al.* KIF5B-RET fusions in lung adenocarcinoma. *Nat Med* 2012; **18**: 375–7.
12 Li F, Feng Y, Fang R *et al.* Identification of *RET* gene fusion by exon array analyses in "pan-negative" lung cancer from never smokers. *Cell Res* 2012; **22**: 928–31.
13 Lipson D, Capelletti M, Yelensky R *et al.* Identification of new *ALK* and *RET* gene fusions from colorectal and lung cancer biopsies. *Nat Med* 2012; **18**: 382–4.
14 Takeuchi K, Soda M, Togashi Y *et al.* RET, ROS1 and ALK fusions in lung cancer. *Nat Med* 2012; **18**: 378–81.
15 Wang R, Hu H, Pan Y *et al.* RET fusions define a unique molecular and clinicopathologic subtype of non-small-cell lung cancer. *J Clin Oncol* 2012; **30**: 4352–9.
16 Gardner E, Papi L, Easton DF *et al.* Genetic linkage studies map the multiple endocrine neoplasia type 2 loci to a small interval on chromosome 10q11.2. *Hum Mol Genet* 1993; **2**: 241–6.
17 Mole SE, Mulligan LM, Healey CS, Ponder BA, Tunnacliffe A. Localisation of the gene for multiple endocrine neoplasia type 2A to a 480 kb region in chromosome band 10q11.2. *Hum Mol Genet* 1993; **2**: 247–52.
18 Mulligan LM, Kwok JB, Healey CS *et al.* Germ-line mutations of the RET proto-oncogene in multiple endocrine neoplasia type 2A. *Nature* 1993; **363**: 458–60.
19 Hofstra RM, Landsvater RM, Ceccherini I *et al.* A mutation in the RET proto-oncogene associated with multiple endocrine neoplasia type 2B and sporadic medullary thyroid carcinoma. *Nature* 1994; **367**: 375–6.
20 Grieco M, Cerrato A, Santoro M, Fusco A, Melillo RM, Vecchio G. Cloning and characterization of H4 (D10S170), a gene involved in RET rearrangements *in vivo*. *Oncogene* 1994; **9**: 2531–5.
21 Matsubara D, Kanai Y, Ishikawa S *et al.* Identification of CCDC6-RET fusion in the human lung adenocarcinoma cell line, LC-2/ad. *J Thorac Oncol* 2012; **7**: 1872–6.
22 Makinoshima H, Ishii G, Kojima M *et al.* PTPRZ1 regulates calmodulin phosphorylation and tumor progression in small-cell lung carcinoma. *BMC Cancer* 2012; **12**: 537.
23 Kataoka H, Itoh H, Seguchi K, Koono M. Establishment and characterization of a human lung adenocarcinoma cell line (LC-2/ad) producing alpha 1-antitrypsin *in vitro*. *Acta Pathol Jpn* 1993; **43**: 566–73.
24 Wedge SR, Ogilvie DJ, Dukes M *et al.* ZD6474 inhibits vascular endothelial growth factor signaling, angiogenesis, and tumor growth following oral administration. *Cancer Res* 2002; **62**: 4645–55.
25 Yoshida A, Tsuta K, Nakamura H *et al.* Comprehensive histologic analysis of ALK-rearranged lung carcinomas. *Am J Surg Pathol* 2011; **35**: 1226–34.
26 Okayama H, Kohno T, Ishii Y *et al.* Identification of genes upregulated in ALK-positive and EGFR/KRAS/ALK-negative lung adenocarcinomas. *Cancer Res* 2012; **72**: 100–11.
27 Ju YS, Lee WC, Shin JY *et al.* A transforming *KIF5B* and *RET* gene fusion in lung adenocarcinoma revealed from whole-genome and transcriptome sequencing. *Genome Res* 2012; **22**: 436–45.
28 Blanco R, Iwakawa R, Tang M *et al.* A gene-alteration profile of human lung cancer cell lines. *Hum Mutat* 2009; **30**: 1199–206.
29 Phay JE, Shah MH. Targeting RET receptor tyrosine kinase activation in cancer. *Clin Cancer Res* 2010; **16**: 5936–41.
30 Antonelli A, Fallahi P, Ferrari SM *et al.* RET TKI: potential role in thyroid cancers. *Curr Oncol Rep* 2012; **14**: 97–104.
31 Scagliotti GV. Potential role of multi-targeted tyrosine kinase inhibitors in non-small-cell lung cancer. *Ann Oncol* 2007; **18**(Suppl 10): x32–41.
32 Couto JP, Almeida A, Daly L *et al.* AZD1480 blocks growth and tumorigenesis of RET- activated thyroid cancer cell lines. *PLoS ONE* 2012; **7**: e46869.
33 Dar AC, Das TK, Shokat KM, Cagan RL. Chemical genetic discovery of targets and anti-targets for cancer polypharmacology. *Nature* 2012; **486**: 80–4.

## Supporting Information

Additional Supporting Information may be found in the online version of this article:

**Data S1.** Materials and methods.

**Fig. S1.** The absence of the known driver mutations.

**Fig. S2.** Suppression of *RET* mRNA in siRET-treated cells.

**Fig. S3.** RET-dependent transcriptome profile in LC-2/ad cells.

**Fig. S4.** Dose-dependent effect of vandetanib in PC-9 cells.

**Fig. S5.** WST-8 assay with various kinase inhibitors.

**Fig. S6.** Effect of sunitinib and sorafenib on G1 phase population of LC-2/ad cells.

**Fig. S7.** Effect of sunitinib and sorafenib on apoptosis of LC-2/ad cells.

**Fig. S8.** Dose-dependent effect of AZD6244 and BEZ235 in LC-2/ad cells.

**Fig. S9.** WST-8 assay of LC-2/ad cells treated with AZD6244 and BEZ235.

**Fig. S10.** Body weight of the vandetanib-, sunitinib-, sorafenib- and vehicle-treated mice.

**Fig. S11.** Effect of sunitinib and sorafenib *in vivo*.

**Table S1.** Polymerase chain reaction primers.

**Table S2.** Summary of the microarray data.

# Identification and Characterization of Cancer Mutations in Japanese Lung Adenocarcinoma without Sequencing of Normal Tissue Counterparts

**Ayako Suzuki[1☯], Sachiyo Mimaki[2☯], Yuki Yamane[3], Akikazu Kawase[3], Koutatsu Matsushima[2], Makito Suzuki[2], Koichi Goto[3], Sumio Sugano[1], Hiroyasu Esumi[2], Yutaka Suzuki[1*], Katsuya Tsuchihara[2]**

**1** Department of Medical Genome Sciences, Graduate School of Frontier Sciences, The University of Tokyo, Chiba, Japan, **2** Division of Translational Research, Research Center for Innovative Oncology, National Cancer Center Hospital East, Chiba, Japan, **3** Thoracic Oncology Division, National Cancer Center Hospital East, Chiba, Japan

## Abstract

We analyzed whole-exome sequencing data from 97 Japanese lung adenocarcinoma patients and identified several putative cancer-related genes and pathways. Particularly, we observed that cancer-related mutation patterns were significantly different between different ethnic groups. As previously reported, mutations in the EGFR gene were characteristic to Japanese, while those in the KRAS gene were more frequent in Caucasians. Furthermore, during the course of this analysis, we found that cancer-specific somatic mutations can be detected without sequencing normal tissue counterparts. 64% of the germline variants could be excluded using a total of 217 external Japanese exome datasets. We also show that a similar approach may be used for other three ethnic groups, although the discriminative power depends on the ethnic group. We demonstrate that the ATM gene and the PAPPA2 gene could be identified as cancer prognosis related genes. By bypassing the sequencing of normal tissue counterparts, this approach provides a useful means of not only reducing the time and cost of sequencing but also analyzing archive samples, for which normal tissue counterparts are not available.

**Citation:** Suzuki A, Mimaki S, Yamane Y, Kawase A, Matsushima K, et al. (2013) Identification and Characterization of Cancer Mutations in Japanese Lung Adenocarcinoma without Sequencing of Normal Tissue Counterparts. PLoS ONE 8(9): e73484. doi:10.1371/journal.pone.0073484

**Editor:** H. Sunny Sun, Institute of Molecular Medicine, Taiwan

**Received** March 22, 2013; **Accepted** July 19, 2013; **Published** September 12, 2013



**Funding:** This work was supported by JSPS KAKENHI Grant number 24300345. This work was also supported by MEXT KAKENHI Grant Number 221S0002. The funders had no role in study design, data collection and analysis, decision to publish, or preparation of the manuscript.

**Competing interests:** The authors have declared that no competing interests exist.

* E-mail: ysuzuki@hgc.jp

☯ These authors contributed equally to this work.

## Introduction

The advent of next generation sequencing technology has greatly facilitated the detection and characterization of genetic variations in the human genome. Most remarkably, this type of study has driven the 1000 Genomes Project [1,2], which aims to provide a comprehensive map of human genetic variants across various ethnic backgrounds. However, because whole-genome sequencing is still costly, the sequencing of whole exon regions using hybridization capture methods (exome sequencing) [3-5] is widely used to screen for genes that are related to hereditary diseases. By sequencing exomes from healthy and diseased individuals and comparing them, genes that are responsible for many diseases have been identified [6], including Miller syndrome [7,8] and familial hyperkalemic hypertension [9]. Along with the progress that has been made in exome sequencing, the volume of germline single nucleotide polymorphism (SNP) data that has been registered in dbSNP is rapidly expanding for various populations [10].

Exome sequencing provides a powerful tool for cancer studies as well. Indeed, a number of papers have been published describing the identification and characterization of single nucleotide variants (SNVs) that somatically occur in cancers and are suspected to be responsible for carcinogenesis and disease development [11]. The International Cancer Genome Consortium (ICGC) has been collecting exome data for somatic SNVs that are present in more than 50 types of cancers as a part of an international collaborative effort [12-14]. The Cancer Genome Atlas (TCGA) has developed a large genomic dataset, including exomes for high-grade ovarian carcinoma, that has been used to detect significantly mutated genes, including TP53, BRCA1 and BRCA2 [15]. They have also identified various genomic aberrations and deregulated pathways that may act as therapeutic targets.